Heavy-to-light form factors to three loops

Matteo Fael,[1] Tobias Huber,[2] Fabian Lange,[3,4] Jakob Müller,[2] Kay Schönwald,[3] and Matthias Steinhauser[5]

[1]*Theoretical Physics Department, CERN, 1211 Geneva, Switzerland*
[2]*Theoretische Physik 1, Center for Particle Physics Siegen (CPPS), Universität Siegen, Walter-Flex-Straße 3, D-57068 Siegen, Germany*
[3]*Physik-Institut, Universität Zürich, Winterthurerstrasse 190, 8057 Zürich, Switzerland*
[4]*Paul Scherrer Institut, 5232 Villigen PSI, Switzerland*
[5]*Institut für Theoretische Teilchenphysik, Karlsruhe Institute of Technology (KIT), 76128 Karlsruhe, Germany*

(Received 18 June 2024; accepted 5 August 2024; published 6 September 2024)

We compute three-loop corrections of $\mathcal{O}(\alpha_s^3)$ to form factors with one massive and one massless quark coupling to an external vector, axialvector, scalar, pseudoscalar, or tensor current. We obtain analytic results for the color-planar contributions, for the contributions of light-quark loops, and the contributions with two heavy-quark loops. For the computation of the remaining master integrals we use the "expand and match" approach which leads to semianalytic results for the form factors. We implement our results in a *Mathematica* and a Fortran code which allows for fast and precise numerical evaluations in the physically relevant phase space. The form factors are used to compute the hard matching coefficients in Soft-Collinear Effective Theory for all currents. The tensor coefficients at lightlike momentum transfer are used to extract the hard function in $\bar{B} \to X_s\gamma$ to three loops.

DOI: 10.1103/PhysRevD.110.056011

I. INTRODUCTION

Form factors are the basic building blocks of scattering amplitudes in quantum field theories. Most prominently, they represent the bulk of virtual corrections to physical observables. The form factors for two massless external particles coupling to an external current have been computed up to four-loop order in QCD and QED for various combinations of particles and currents [1–19]. The heavy quark form factors, i.e. two fermions with the same mass coupling to a current, were known at the two-loop level for a long time [20–32] and partial three-loop results became available over the last decade [29,32–37]. Recently, the three-loop corrections for the vector, axialvector, scalar, and pseudoscalar currents were completed semianalytically [38–40].

The heavy-to-light form factors of a heavy and a light fermion are especially relevant for decays of heavy quarks such as $t \to bW^*$, $b \to cW^*$, and $b \to uW^*$ or the production of a single top quark through the t-channel process. Specializing to QED, they also contribute to the muon decay in the Fermi theory, see e.g. Refs. [41,42]. For some of the applications, neglecting the mass of the light fermion is a good first approximation in which the form factors were known to two-loop order for some time [43–46].[1] Only a few years ago the full mass dependence of the heavy-to-light form factor became available at $\mathcal{O}(\alpha_s^2)$ [50,51]. Neglecting the light fermion mass, the color-planar corrections at $\mathcal{O}(\alpha_s^3)$ to the vector, axialvector, scalar, and pseudoscalar form factors were computed recently [52,53].

In this paper we compute the three-loop corrections to the heavy-to-light form factors in full QCD, still neglecting the mass of the light fermion. We reproduce the analytic results of Ref. [53] in the color-planar limit and extend it to the tensor form factors. Furthermore, we provide analytic results for the contributions of light-fermion loops and the contributions with two heavy-fermion loops for all form factors. For the remaining color factors we present semianalytic results in terms of expansions around kinematic points following the strategy of Ref. [54] which was already applied to the three-loop corrections to the massive form factors in Refs. [38–40]. We restrict ourselves to the physically interesting regions relevant for the heavy-fermion decay and the heavy-fermion production in the t-channel. Furthermore, we present results for generic external currents. The specification to vertices appearing in the Standard Model or other theories of interest is

[1]See also Refs. [47–49] for the computation of the respective master integrals.

straightforward. We provide our analytic results in the form of ancillary files accompanying this paper, and the numeric results for the full form factors as *Mathematica* and Fortran programs which perform an interpolation based on a dense grid [55].

The QCD form factors can be used to compute the hard matching coefficients to Soft-Collinear Effective theory (SCET) [56–59] at leading power in the SCET expansion. The infrared divergences still present in the QCD form factors are removed during the procedure of infrared subtraction, yielding finite SCET matching coefficients. While their one-loop expressions have been computed in the founding SCET papers (see also Ref. [60]), the two-loop coefficients for the vector and axial vector current were computed in Refs. [43–46]. In Ref. [61] the results were extended to the scalar and tensor currents. In the present paper the matching coefficients are computed to three-loop order for all currents considered.

An immediate application of the matching coefficients of the tensor current at lightlike momentum transfer concerns the inclusive decay $\bar{B} \to X_s\gamma$. In a SCET-based approach, the decay rate is formulated in a factorized form as the product of a hard function times a convolution of a jet with a soft function [62–64]. While the latter two are known to three loops already [65–68], the hard function has to date only been evaluated to two loops [69–71]. With the three-loop matching coefficients at hand we close this gap and compute the three-loop QCD correction to the hard function in $\bar{B} \to X_s\gamma$.

In the recent study [71], the authors claim the performance of a next-to-next-to-next-to-leading-logarithmic analysis of the photon energy spectrum in $\bar{B} \to X_s\gamma$ including three-loop corrections to the renormalization-scale independent part of the hard, jet, and soft functions in SCET (i.e. a study to $\mathrm{N^3LL'}$ accuracy). However, for the hard function this piece has only become available with the calculation presented here. In Ref. [71] the missing numerical coefficient at three loops was treated as a nuisance parameter. Our explicit three-loop calculation shows that the exact numerical value of the parameter in question lies more than a factor of two outside the variation region assumed in Ref. [71].

The remainder of this paper is structured as follows: In Sec. II we introduce the form factors and discuss their renormalization, the infrared subtraction, as well as the Ward identities of the currents which relate some of the form factors. Our calculational strategy is described in Sec. III. We then present our results and discuss the analytic and numeric results in Secs. IV and V, respectively. The hard function in $\bar{B} \to X_s\gamma$ is presented in Sec. VI. We conclude in Sec. VII. In the Appendixes we present explicit results for the projectors to all form factors. Furthermore, we describe the program FFh2l where our results are implemented and which allows for a fast and precise numerical evaluation.

II. FORM FACTORS

A. Currents and form factors

The theoretical framework used for our calculation is QCD supplemented with external currents formed by a heavy (Q) and a light quark field (q). In this paper we consider the vector, axialvector, scalar, pseudoscalar, and tensor currents

$$\begin{aligned} j^v_\mu &= \bar{\psi}_Q \gamma_\mu \psi_q, \\ j^a_\mu &= \bar{\psi}_Q \gamma_\mu \gamma_5 \psi_q, \\ j^s &= \bar{\psi}_Q \psi_q, \\ j^p &= \mathrm{i}\bar{\psi}_Q \gamma_5 \psi_q, \\ j^t_{\mu\nu} &= \mathrm{i}\bar{\psi}_Q \sigma_{\mu\nu} \psi_q, \end{aligned} \tag{1}$$

where $\sigma_{\mu\nu} = \mathrm{i}[\gamma^\mu, \gamma^\nu]/2$ is antisymmetric in the indices μ and ν. The wave functions of the heavy and light quark fields are denoted by ψ_Q and ψ_q, respectively. We use the currents from Eq. (1) to construct vertex functions $\Gamma(q_1, q_2)$ via

$$\int \frac{\mathrm{d}^4 y}{(2\pi)^4} \mathrm{e}^{\mathrm{i}q\cdot y} \langle \psi^{\mathrm{out}}_Q(q_2, s_2) | j^x(y) | \psi^{\mathrm{in}}_q(q_1, s_1) \rangle = \bar{u}(q_2, s_2) \Gamma(q_1, q_2) u(q_1, s_1) \delta^{(4)}(q - q_1 - q_2), \tag{2}$$

which are independent of the spin indices s_1 and s_2 and which can be decomposed into scalar form factors. We follow the notation introduced in Ref. [39] and define them as

$$\begin{aligned} \Gamma^v_\mu(q_1, q_2) &= F^v_1(q^2)\gamma_\mu - \frac{\mathrm{i}}{m} F^v_2(q^2)\sigma_{\mu\nu}q^\nu + \frac{2}{m} F^v_3(q^2) q_\mu, \\ \Gamma^a_\mu(q_1, q_2) &= F^a_1(q^2)\gamma_\mu\gamma_5 - \frac{\mathrm{i}}{m} F^a_2(q^2)\sigma_{\mu\nu}q^\nu\gamma_5 + \frac{2}{m} F^a_3(q^2) q_\mu\gamma_5, \\ \Gamma^s(q_1, q_2) &= F^s(q^2), \\ \Gamma^p(q_1, q_2) &= \mathrm{i}F^p(q^2)\gamma_5, \\ \Gamma^t_{\mu\nu}(q_1, q_2) &= \mathrm{i}F^t_1(q^2)\sigma_{\mu\nu} + \frac{F^t_2(q^2)}{m}(q_{1,\mu}\gamma_\nu - q_{1,\nu}\gamma_\mu) + \frac{F^t_3(q^2)}{m}(q_{2,\mu}\gamma_\nu - q_{2,\nu}\gamma_\mu) + \frac{F^t_4(q^2)}{m^2}(q_{1,\mu}q_{2,\nu} - q_{1,\nu}q_{2,\mu}). \end{aligned} \tag{3}$$

Here, q_1 is the incoming momentum of the massless quark and q_2 is the outgoing momentum of the heavy quark. Furthermore, we have $q = q_1 - q_2$, with $q^2 = s$, $q_1^2 = 0$, and $q_2^2 = m^2$. In all vertex functions the color structure is a simple Kronecker delta in the fundamental color indices of the external quarks and is not written out explicitly.

For the perturbative expansion of the scalar form factors we introduce

$$F = \sum_{i\geq 0} \left(\frac{\alpha_s(\mu)}{\pi}\right)^i F^{(i)}, \tag{4}$$

where α_s depends on the number of active flavors. We will use $\alpha_s^{(n_l)}$ (with $n_f = n_l + n_h$) for the parametrization of the ultraviolet renormalized but still infrared divergent form factors and for the finite matching coefficients where also the infrared divergences have been subtracted. Here, n_f is the number of active flavors, i.e. for the $b \to u$ vertex corrections we have $n_f = 5$ with $n_h = 1$. The nonzero tree-level contributions are given by

$$F_1^{v,(0)} = F_1^{a,(0)} = F^{s,(0)} = F^{p,(0)} = F_1^{t,(0)} = 1. \tag{5}$$

The form factors of the heavy-light currents do not get contributions from so-called singlet diagrams where the external current couples to a closed quark loop. This allows us to use anticommuting γ_5 without ambiguity. Since one of the quarks is massless it is always possible to anticommute γ_5 to one end of the fermion string and obtain simple relations for the axialvector and pseudoscalar form factors to their vector and scalar counterparts. In our case we have

$$F_1^a = F_1^v, \qquad F_2^a = F_2^v, \qquad F_3^a = F_3^v, \qquad F^s = F^p. \tag{6}$$

We use these relations as an internal cross-check for our calculation.

In the work [53] the vector and axialvector form factors have been considered with a slightly different decomposition of the vertex functions. The authors have introduced scalar factors G_1, G_2, and G_3 which are related to ours via

$$F_1^v = G_1 + \frac{1}{2}G_2, \qquad F_2^v = -\frac{1}{2}G_2, \qquad F_3^v = -\frac{1}{4}G_3. \tag{7}$$

B. Renormalization

For the three-loop calculation of the form factors we have to perform the standard parameter renormalization of the strong coupling and the quark masses, the wave function renormalization of the massive and massless external quarks, and the renormalization of the external currents. Furthermore, we decouple the contribution from the heavy quark from the running of α_s. Then the combination with the subtraction terms from the infrared divergences is more convenient. We thus write the ultraviolet renormalized form factors as

$$F^x = Z_x (Z_{2,Q}^{\mathrm{OS}})^{1/2} (Z_{2,q}^{\mathrm{OS}})^{1/2} F^{x,\mathrm{bare}} \Big|_{\alpha_s^{\mathrm{bare}} = Z_{\alpha_s} \alpha_s^{(n_f)}, m^{\mathrm{bare}} = Z_m^{\mathrm{OS}} m^{\mathrm{OS}}, \alpha_s^{(n_f)} = \zeta_{\alpha_s}^{-1} \alpha_s^{(n_l)}}. \tag{8}$$

The bare one-loop vertex corrections develop $1/\epsilon^2$ terms and at two-loop order we even have quartic poles. Thus the (on-shell) renormalization and decoupling constants are required to order ϵ^4 at one-loop order and to order ϵ^2 at two loops.

Let us summarize the renormalization constants appearing in Eq. (8), up to which orders they are needed, and which schemes we choose:

(i) The renormalization of α_s is needed to two-loop order and is performed in the $\overline{\mathrm{MS}}$ scheme [72–74].

(ii) The renormalization of the heavy-quark mass m is required to two-loop order. We choose the on-shell scheme [75,76], in which we need the one-loop result to order ϵ^4 and the two-loop result to order ϵ^2 [77–80].

(iii) The on-shell wave function renormalization constant of the heavy quark, $Z_{2,Q}^{\mathrm{OS}}$, is needed to three-loop order and can be found in Refs. [81–83]. Again, we need the one-loop result to order ϵ^4 and the two-loop result to order ϵ^2 [84].

(iv) The wave function renormalization constant of the light quark, $Z_{2,q}^{\mathrm{OS}}$, starts at order α_s^2 and is needed up to three-loop order [85]. We need the two-loop result to order ϵ^2 [86].

(v) Since the vector and axialvector current are conserved, their anomalous dimensions vanish and we have $Z_v = Z_a = 1$.

(vi) The anomalous dimension of the scalar and pseudoscalar currents corresponds to the anomalous dimension of the quark mass and we thus have $Z_s = Z_p = Z_m$, which we need to three loops. We choose to renormalize it both in the $\overline{\mathrm{MS}}$ as well as in the on-shell scheme. $Z_m^{\overline{\mathrm{MS}}}$ is available from Refs. [75,87,88]. For Z_m^{OS}, we again need the one-loop result to order ϵ^4 and the two-loop result to order ϵ^2 [75–80].

(vii) The tensor current has a nonvanishing anomalous dimension which cannot be deduced from other quantities. We need it to three loops to construct Z_t in the $\overline{\mathrm{MS}}$ scheme [89,90].

(viii) Finally, we decouple the heavy quark(s) from the running by employing the decoupling relation $\alpha_s^{(n_f)} = \zeta_{\alpha_s}^{-1}\alpha_s^{(n_l)}$, where we remind the reader that $n_f = n_l + n_h$. We require the decoupling relation to two loops [85,91–96], the one-loop result to order ϵ^4, and the two-loop result to order ϵ^2 [85,86,97–100].

C. Ward identities

Using the equations of motion, one can derive the Ward identities

$$\begin{aligned}\partial^\mu j_\mu^v &= \mathrm{i}m j^s,\\ \partial^\mu j_\mu^a &= m j^p\end{aligned} \tag{9}$$

between the renormalized vector and scalar as well as between the axialvector and pseudoscalar currents. The equations of motion imply that both the mass and the currents are renormalized in the on-shell scheme. Due to Eq. (6) it is sufficient to consider the vector and the scalar currents in the following. Employing Eq. (2), we can rewrite the Ward identity as

$$-q^\mu \Gamma_\mu^v = m\Gamma^s \tag{10}$$

on the level of the renormalized vertices (see e.g. Ref. [43]). Using Eq. (3) then leads to the relation

$$F_1^v - \frac{2s}{m^2}F_3^v = F^s \tag{11}$$

between the renormalized form factors. This provides an important check on our results later, which we discuss in Sec. V.

D. Infrared subtraction and matching onto SCET

Infrared singularities of multileg QCD amplitudes with a massive and massless partons have been discussed in Refs. [101,102]. By specifying ourselves to the case $Q \to q$, i.e. one massive initial quark and one massless final state quark, we can write the Z factor associated to the infrared subtraction in the minimal scheme in the following way:

$$\begin{aligned}\ln Z = {}& \frac{\alpha_s}{4\pi}\left[\frac{\Gamma_0'}{4\epsilon^2} + \frac{\Gamma_0}{2\epsilon}\right] + \left(\frac{\alpha_s}{4\pi}\right)^2\left[-\frac{3\beta_0\Gamma_0'}{16\epsilon^3} + \frac{\Gamma_1' - 4\beta_0\Gamma_0}{16\epsilon^2} + \frac{\Gamma_1}{4\epsilon}\right]\\ &+ \left(\frac{\alpha_s}{4\pi}\right)^3\left[\frac{11\beta_0^2\Gamma_0'}{72\epsilon^4} - \frac{5\beta_0\Gamma_1' + 8\beta_1\Gamma_0' - 12\beta_0^2\Gamma_0}{72\epsilon^3} + \frac{\Gamma_2' - 6\beta_0\Gamma_1 - 6\beta_1\Gamma_0}{36\epsilon^2} + \frac{\Gamma_2}{6\epsilon}\right] + \mathcal{O}(\alpha_s^4),\end{aligned} \tag{12}$$

where $\alpha_s \equiv \alpha_s^{(n_l)}(\mu)$,

$$\Gamma = \gamma^Q(\alpha_s) + \gamma^q(\alpha_s) - \gamma^{\mathrm{cusp}}(\alpha_s)\log\left(\frac{\mu}{m(1-x)}\right) = \sum_{n=0}^{\infty}\Gamma_n\left(\frac{\alpha_s}{4\pi}\right)^{n+1} \tag{13}$$

with $x = s/m^2$ and

$$\Gamma' = \frac{\partial}{\partial\log\mu}\Gamma = -\gamma^{\mathrm{cusp}}(\alpha_s). \tag{14}$$

The coefficients in the perturbative series of the lightlike cusp anomalous dimension

$$\gamma^{\mathrm{cusp}}(\alpha_s) = \sum_{n=0}^{\infty}\gamma_n^{\mathrm{cusp}}\left(\frac{\alpha_s}{4\pi}\right)^{n+1} \tag{15}$$

are available up to four-loop order [9,11–14,16,103–110]. Up to three loops we have

$$\begin{aligned}\gamma_0^{\mathrm{cusp}} &= 4C_F,\\ \gamma_1^{\mathrm{cusp}} &= 4C_F\left[C_A\left(\frac{67}{9} - \frac{\pi^2}{3}\right) - \frac{20}{9}T_F n_l\right],\\ \gamma_2^{\mathrm{cusp}} &= 4C_F\left[C_A^2\left(\frac{245}{6} - \frac{134\pi^2}{27} + \frac{22\zeta_3}{3} + \frac{11\pi^4}{45}\right) + C_F T_F n_l\left(16\zeta_3 - \frac{55}{3}\right)\right.\\ &\quad \left. + C_A T_F n_l\left(-\frac{418}{27} + \frac{40\pi^2}{27} - \frac{56\zeta_3}{3}\right) - \frac{16}{27}T_F^2 n_l^2\right].\end{aligned} \tag{16}$$

The perturbative expansion of the anomalous dimension γ^i (for $i = q, Q$) can be written as

$$\gamma^i(\alpha_s) = \sum_{n=0}^{\infty} \gamma_n^i \left(\frac{\alpha_s}{4\pi}\right)^{n+1} \tag{17}$$

and it can be extracted from the divergent part of the quark form factor. γ^q is know to four-loop order [5,16,110–112]; up to three loops the results read:

$$\begin{aligned}
\gamma_0^q &= -3C_F, \\
\gamma_1^q &= C_A C_F\left(-\frac{961}{54} - \frac{11\pi^2}{6} + 26\zeta_3\right) + C_F^2\left(-\frac{3}{2} + 2\pi^2 - 24\zeta_3\right) + C_F n_l T_F\left(\frac{130}{27} + \frac{2\pi^2}{3}\right), \\
\gamma_2^q &= C_A^2 C_F\left(-\frac{139345}{2916} - \frac{7163\pi^2}{486} + \frac{3526\zeta_3}{9} - \frac{83\pi^4}{90} - \frac{44\pi^2\zeta_3}{9} - 136\zeta_5\right) \\
&\quad + C_A C_F^2\left(-\frac{151}{4} + \frac{205\pi^2}{9} - \frac{844\zeta_3}{3} + \frac{247\pi^4}{135} - \frac{8\pi^2\zeta_3}{3} - 120\zeta_5\right) + C_F^3\left(-\frac{29}{2} - 3\pi^2 - 68\zeta_3 - \frac{8\pi^4}{5} + 240\zeta_5 + \frac{16\pi^2\zeta_3}{3}\right) \\
&\quad + C_A C_F T_F n_l\left(-\frac{17318}{729} + \frac{2594\pi^2}{243} - \frac{1928\zeta_3}{27} + \frac{22\pi^4}{45}\right) \\
&\quad + C_F^2 T_F n_l\left(\frac{2953}{27} - \frac{26\pi^2}{9} + \frac{512\zeta_3}{9} - \frac{28\pi^4}{27}\right) + C_F T_F^2 n_l^2\left(\frac{9668}{729} - \frac{40\pi^2}{27} - \frac{32\zeta_3}{27}\right).
\end{aligned} \tag{18}$$

For massive quarks, γ^Q is available up to three loops [68,113–117]:

$$\begin{aligned}
\gamma_0^Q &= -2C_F, \\
\gamma_1^Q &= C_A C_F\left(-\frac{98}{9} + \frac{2\pi^2}{3} - 4\zeta_3\right) + \frac{40}{9} C_F T_F n_l, \\
\gamma_2^Q &= C_A^2 C_F\left(-\frac{343}{9} + \frac{304\pi^2}{27} - \frac{740\zeta_3}{9} - \frac{22\pi^4}{45} - \frac{4\pi^2\zeta_3}{3} + 36\zeta_5\right) + C_A C_F T_F n_l\left(+\frac{356}{27} - \frac{80\pi^2}{27}\frac{496\zeta_3}{9}\right) \\
&\quad + C_F^2 T_F n_l\left(\frac{110}{3} - 32\zeta_3\right) + \frac{32}{27} C_F T_F^2 n_l^2.
\end{aligned} \tag{19}$$

Note that Z introduced in Eq. (12) is defined in terms of $\alpha_s^{(n_l)}$. Thus, the decoupling relation has to be applied to the form factors in d dimensions as discussed in the previous section. We then have

$$C = Z^{-1} F, \tag{20}$$

where F is any of the ultraviolet renormalized form factors. The corresponding matching coefficient C is finite (i.e. the limit $\epsilon \to 0$ can be taken), and expanded perturbatively in analogy to Eq. (4). Note that C_3^t and C_4^t vanish in four dimensions since the pseudotensor current is reducible in four space-time dimensions. This serves as another nontrivial check of our calculation.

Like Z, the matching coefficients C are expanded in $\alpha_s^{(n_l)}(\mu)$. They satisfy the renormalization group equation (RGE)

$$\frac{d}{d\ln(\mu)} C(s,\mu) = \left[\gamma^{\text{cusp}}(\alpha_s^{(n_l)}) \ln\left(\frac{(1-x)m}{\mu}\right) + \gamma^H(\alpha_s^{(n_l)}) + \gamma^{\text{QCD}}(\alpha_s^{(n_f)})\right] C(s,\mu), \tag{21}$$

with $\gamma^H = \gamma^Q + \gamma^q$. The quantity γ^{QCD} is the anomalous dimension of the corresponding QCD current. It is expanded in $\alpha_s^{(n_f)}$ and can be extracted from the general formula [90][2]

[2]Note the typo in Eq. (7) of Ref. [90]: $-144 T_F^2 C_F^2$ should read $-144 T_F^2 n_f^2$, in accordance with Eq. (6) of Ref. [90].

$$\gamma_{(n)} = -(n-1)(n-3)C_F\left(\frac{\alpha_s^{(n_f)}}{4\pi}\right) + [4(n-15)T_F n_f + (18n^3 - 126n^2 + 163n + 291)C_A$$
$$- 9(n-3)(5n^2 - 20n + 1)C_F]\frac{(n-1)}{18}C_F\left(\frac{\alpha_s^{(n_f)}}{4\pi}\right)^2 + \{[144n^5 - 1584n^4 + 6810n^3 - 15846n^2 + 15933n + 11413$$
$$- 216n(n-3)(n-4)(2n^2 - 8n + 13)\zeta_3)]C_A^2 - [3(72n^5 - 792n^4 + 3809n^3 - 11279n^2 + 15337n + 1161)$$
$$- 432n(n-3)(n-4)(3n^2 - 12n + 19)\zeta_3]C_A C_F - [18(n-3)(17n^4 - 136n^3 + 281n^2 - 36n + 129)$$
$$+ 864n(n-3)(n-4)(n^2 - 4n + 6)\zeta_3]C_F^2 + [8(3n^3 + 51n^2 - 226n - 278)$$
$$+ 1728(n-3)\zeta_3]C_A T_F n_f - [12(17n^3 + n^2 - 326n + 414) + 1728(n-3)\zeta_3]C_F T_F n_f$$
$$+ 16(13n - 35)T_F^2 n_f^2\}\frac{(n-1)}{108}C_F\left(\frac{\alpha_s^{(n_f)}}{4\pi}\right)^3 + \mathcal{O}(\alpha_s^4) \tag{22}$$

via $\gamma^{\rm QCD}_{\{s,v,t\}} = -2\gamma_{\{(0),(1),(2)\}}$, where $\gamma_{(1)} = 0$ due to the conservation of the vector current.

The structure in Eq. (21) allows us to distinguish two scales; the scale μ that governs the renormalization group evolution in SCET, and a second scale ν that governs the renormalization group evolution in QCD. The matching coefficients $C(s,\mu,\nu)$ then fulfill the two separate RGEs

$$\frac{d}{d\ln(\mu)}C(s,\mu,\nu) = \left[\gamma^{\rm cusp}(\alpha_s^{(n_l)}(\mu))\ln\left(\frac{(1-x)m}{\mu}\right) + \gamma^H(\alpha_s^{(n_l)}(\mu))\right]C(s,\mu,\nu), \tag{23}$$

$$\frac{d}{d\ln(\nu)}C(s,\mu,\nu) = \gamma^{\rm QCD}(\alpha_s^{(n_f)}(\nu))C(s,\mu,\nu). \tag{24}$$

The dependence of the matching coefficients on $L_\mu = \ln(\mu^2/m^2)$ and $L_\nu = \ln(\nu^2/m^2)$ is then most conveniently derived by combining the running and the decoupling relation,

$$\alpha_s^{(n_f)}(\nu) = \alpha_s^{(n_f)}(\mu)\left[1 - \beta_0^{(n_f)}\ln\left(\frac{\nu^2}{\mu^2}\right)\left(\frac{\alpha_s^{(n_f)}(\mu)}{4\pi}\right)\right.$$
$$\left. + \left(\beta_0^{(n_f)2}\ln^2\left(\frac{\nu^2}{\mu^2}\right) - \beta_1^{(n_f)}\ln\left(\frac{\nu^2}{\mu^2}\right)\right)\left(\frac{\alpha_s^{(n_f)}(\mu)}{4\pi}\right)^2 + \mathcal{O}(\alpha_s^3)\right], \tag{25}$$

$$\alpha_s^{(n_f)}(\mu) = \alpha_s^{(n_l)}(\mu)\left[1 + \frac{4}{3}L_\mu T_F\left(\frac{\alpha_s^{(n_l)}(\mu)}{4\pi}\right)\right.$$
$$\left. + \left(\frac{16}{9}L_\mu^2 T_F^2 + C_F T_F(4L_\mu + 15) + \frac{4}{9}C_A T_F(15L_\mu - 8)\right)\left(\frac{\alpha_s^{(n_l)}(\mu)}{4\pi}\right)^2 + \mathcal{O}(\alpha_s^3)\right]. \tag{26}$$

Note that contrary to Eq. (20) the four-dimensional version of the decoupling relation is sufficient here. The coefficients of the QCD β function follow from

$$\frac{d\alpha_s^{(n_f)}(\mu)}{d\ln\mu} = -2\alpha_s^{(n_f)}(\mu)\left[\beta_0^{(n_f)}\left(\frac{\alpha_s^{(n_f)}(\mu)}{4\pi}\right) + \beta_1^{(n_f)}\left(\frac{\alpha_s^{(n_f)}(\mu)}{4\pi}\right)^2 + \mathcal{O}(\alpha_s^3)\right] \tag{27}$$

and assume their usual form

$$\beta_0^{(n_f)} = \frac{11}{3}C_A - \frac{4}{3}n_f T_F, \tag{28}$$

$$\beta_1^{(n_f)} = \frac{34}{3}C_A^2 - \frac{20}{3}n_f T_F C_A - 4n_f T_F C_F. \tag{29}$$

III. TECHNICALITIES

For our calculation we use the canonical chain based on QGRAF [118], TAPIR [119], EXP [120,121], the inhouse FORM [122,123] code CALC, Kira [124,125], and FireFly [126,127]. All one- and two-loop and some of the three-loop master integrals are computed to sufficiently high order in ϵ analytically. For the remaining three-loop master integrals we construct semianalytic results based on "expand and match" [38–40,54].

A. Amplitude and projectors

In Fig. 1 we show a set of sample Feynman diagrams for the heavy-to-light form factors.

One of the first steps in our calculation is the application of projectors for the scalar form factors introduced in Eq. (3). Explicit expressions are given in Appendix A. Afterwards there are no open indices and all the scalar products can be decomposed into denominator factors used to define the integral families. For this step we use an auxiliary file generated by TAPIR. In total we have contributions from 47 integral families. We extract the respective lists of integrals which serve as input for the integral reduction. For all external currents we generate the corresponding amplitude for general QCD gauge parameter ξ.

B. Integral reduction

In a next step, we want to reduce the list of integrals contributing to the amplitude to a smaller set of master integrals using integration-by-parts relations [128–130] and the Laporta algorithm [131]. Before performing the actual reduction for the amplitude, we reduce sample integrals with up to two dots and one scalar product for each integral family using Kira [124,125], employing Fermat [132] as computational backend. These samples allow us to find a basis of master integrals in which the dependence on the space-time d and the kinematic variable s/m^2 factorizes in the denominators of all coefficients appearing in the final reduction tables [133,134]. We achieve this as well as a reduction of spurious poles in ϵ with an improved version of the code ImproveMasters.m [133].

With the basis chosen, we then perform the reductions of all integral families again employing Kira, this time

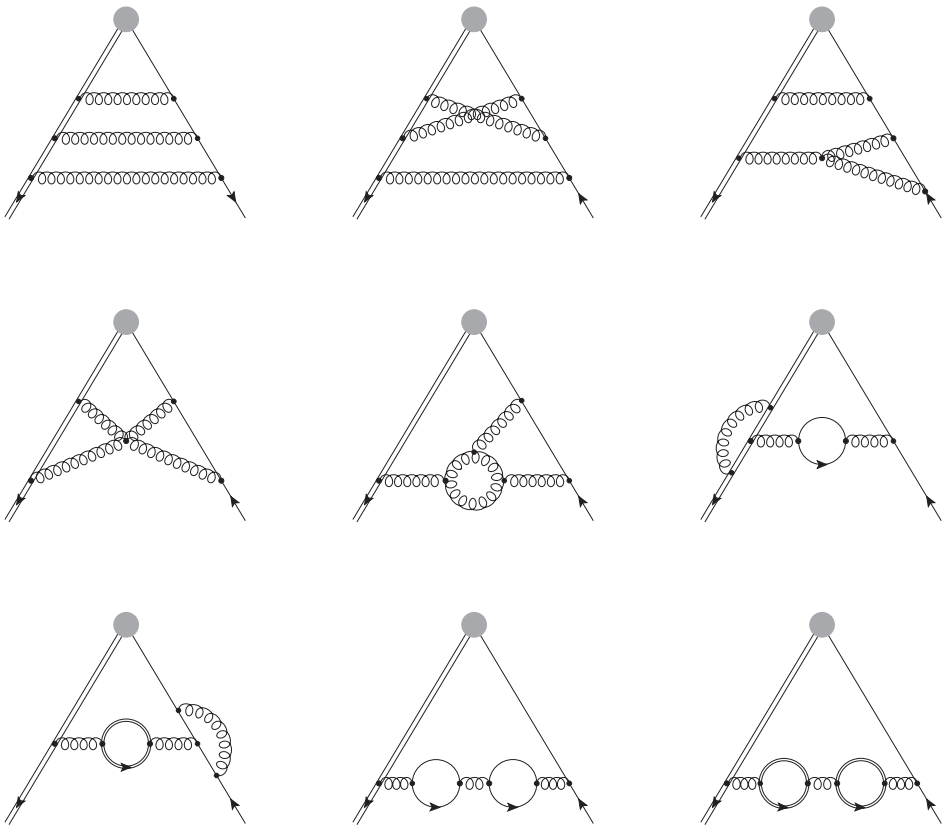

FIG. 1. Sample Feynman diagrams contributing to the heavy-to-light form factors. The double solid, solid, and curly lines refer to massive quarks, massless quarks, and gluons, respectively. The gray blob represents one of the external currents given in Eq. (1).

exploiting the finite field techniques [135–137] implemented in FireFly [126,127].[3] In addition to the separate reductions of all families, we run Kira to find symmetries between the master integrals and arrive at a set of 429 master integrals at the three-loop level. We then use LiteRed [139,140] and a subsequent reduction with Kira and FireFly to establish differential equations for the master integrals [141–144] in s/m^2.

C. Master integrals

We calculate the master integrals at one and two loops analytically. Additionally, we also consider the master integrals which contribute to the leading-color amplitude, the ones depending on the number of light flavors, and the ones with two closed heavy-fermion loops analytically. The master integrals contributing to the leading color amplitude have been obtained before in Refs. [52,53]. In the second reference also the leading color amplitudes for the vector, axialvector, scalar, and pseudoscalar currents have been obtained. We consider in addition the tensor current. For the calculation we use the techniques of Ref. [35]. In practice this means that we do not try to find a canonical basis of master integrals, but we uncouple blocks of the differential equation into higher-order ones and solve these via the factorization of the differential operator and variation of constants. This technique is successful for the considered subset of master integrals since the differential operators factorize to first order and the results can therefore be expressed as iterated integrals over algebraic letters. We checked explicitly that this is not the case for the full amplitude, where also elliptic sectors contribute. For the implementation of the algorithms we make use of the packages Sigma [145,146] and HarmonicSums [147–158].

The boundary constants for the solution are either obtained by direct integration, Mellin-Barnes techniques, or using PSLQ [159] on numerical results computed with AMFLow [160] implementing the auxiliary-mass flow method [161–163] at the point $s = 0$. Many boundary conditions can also be fixed by regularity conditions in $s/m^2 = 0$ and $s/m^2 = 1$.

We find that we can express our analytical results as iterated integrals over the alphabet

$$\frac{1}{x}, \qquad \frac{1}{1 \pm x}, \qquad \frac{1}{2 - x}.$$

For the remaining master integrals we use the semianalytic technique developed in Ref. [38–40,54]. The method is based on series expansions around regular and singular points of the differential equation. Two neighboring expansions are then numerically matched at a point where both expansions converge. We use expansions at the points

$$\begin{aligned}\frac{s}{m^2} = \{&-\infty, -60, -40, -30, -20, -15, -10, -8, -7,\\ &-6, -5, -4, -3, -2, -1, -1/2, 0, 1/4, 1/2,\\ &3/4, 7/8, 1\},\end{aligned} \tag{30}$$

where in each case we used 50 expansion terms. All but the expansions around $s/m^2 = 1$ and $s/m^2 = -\infty$ are regular Taylor expansions. We used boundary conditions at the regular point $s/m^2 = 0$ which we obtained with the help of AMFLow demanding 100 digits precision.

IV. ANALYTICAL RESULTS

As mentioned in Sec. III C, we have analytic results for all one- and two-loop form factors up to order ϵ^4 and ϵ^2, respectively. The computer-readable expressions for all twelve scalar form factors can be downloaded from Ref. [164] for general renormalization scales μ and ν and with the option to renormalize the scalar and pseudoscalar current in the $\overline{\text{MS}}$ or in the on-shell scheme. We provide both expressions where only the ultraviolet counterterms have been introduced, and expressions where in addition the infrared poles have been subtracted. For illustration we show in the following the result for C_1^t for $\nu^2 = \mu^2 = m^2$ up to $\mathcal{O}(\epsilon^0)$ which up to two-loop order reads ($x = s/m^2$):

$$C_1^{t,(0)} = 1,$$

$$C_1^{t,(1)} = C_F\left\{-\frac{3}{2} - \frac{\pi^2}{48} + \frac{(1-2x)H_1}{2x} - \frac{1}{2}H_{0,1} - H_{1,1}\right\},$$

$$\begin{aligned}C_1^{t,(2)} = C_A C_F\Bigg\{&-\frac{119851}{20736} - \frac{\pi^4(-49 + 75x - 201x^2 + 31x^3)}{1920(1-x)^3} + \frac{(354 - 829x)H_1}{216x}\\ &+ \zeta_3\left(\frac{398 - 978x + 681x^2 - 137x^3}{576(1-x)^3} + \frac{7}{8}H_1\right) + \pi^2\left(\frac{253 - 830x - 1007x^2}{3456(1-x)^2}\right.\end{aligned}$$

[3]While we managed to complete the reduction after fixing the gauge to $\xi = 0$ with Kira 2.3, we resorted to the current development version to perform the reduction for general ξ. We thank Johann Usovitsch and Zihao Wu for allowing us to use the development version (see Ref. [138] for a first brief discussion of some of the improvements).

$$
\begin{aligned}
&-\frac{(24-x+56x^2+65x^3)H_1}{288(1-x)^2x}-\frac{(2-x)(2-5x-x^2)H_2}{96(1-x)^3}-\frac{(1+x)(1-3x)H_{-1}}{24(1-x)x}+\frac{(1-15x-6x^2-4x^3)H_{0,1}}{48(1-x)^3}\\
&+\frac{1}{24}H_{0,-1}+\frac{1}{12}H_{1,1}-\frac{(32-48x+9x^2+11x^3)\ln(2)}{96(1-x)^3}\Big)+\frac{(66-308x+259x^2-149x^3)H_{0,1}}{144(1-x)^2x}\\
&+\frac{(2-5x)(39-83x)H_{1,1}}{144(1-x)x}+\frac{(8+12x+9x^2-25x^3)H_{0,0,1}}{48(1-x)^3}-\frac{(20-192x+237x^2-61x^3)H_{0,1,1}}{48(1-x)^3}\\
&-\frac{(15-16x+17x^2)H_{1,0,1}}{16(1-x)^2}-\frac{11}{6}H_{1,1,1}-\frac{(2-x)(2-5x-x^2)H_{2,1,1}}{48(1-x)^3}-\frac{(1+x)(1-3x)H_{-1,0,1}}{2(1-x)x}\\
&+\frac{(1+x+6x^2)H_{0,0,0,1}}{8(1-x)^3}+\frac{(1+x+6x^2)H_{0,0,1,1}}{4(1-x)^3}-\frac{(1+x+6x^2)H_{0,1,0,1}}{8(1-x)^3}+\frac{1}{2}H_{0,-1,0,1}+\frac{1}{2}H_{1,0,0,1}\Big\}\\
&+C_F^2\Big\{\frac{2515}{768}+\frac{\pi^4(389+7473x-1857x^2+907x^3)}{23040(1-x)^3}+H_{1,0,1,1}-\frac{(3-8x)H_1}{4x}-\zeta_3\Big(\frac{26-54x+21x^2+3x^3}{32(1-x)^3}+\frac{1}{2}H_1\Big)\\
&+\pi^2\Big(-\frac{51+47x+2x^2}{48(1-x)^2}+\frac{(11-114x-105x^2+16x^3)H_1}{96(1-x)^2x}+\frac{(2-x)(2-5x-x^2)H_2}{48(1-x)^3}+\frac{(1+x)(1-3x)H_{-1}}{12(1-x)x}\\
&-\frac{(35+135x+21x^2+x^3)H_{0,1}}{96(1-x)^3}-\frac{1}{12}H_{0,-1}+\frac{1}{48}H_{1,1}+\frac{(32-48x+9x^2+11x^3)\ln(2)}{48(1-x)^3}\Big)\\
&-\frac{(6-42x+91x^2+45x^3)H_{0,1}}{24(1-x)^2x}+\frac{(97+3x)H_{1,1}}{24(1-x)}+\frac{(6+12x+84x^2-141x^3+35x^4)H_{0,0,1}}{24(1-x)^3x}\\
&-\frac{3(1-2x)H_{1,1,1}}{2x}-\frac{(12-150x+126x^2-51x^3+59x^4)H_{0,1,1}}{24(1-x)^3x}+\frac{(-41-68x+13x^2)H_{1,0,1}}{24(-1+x)^2}\\
&-\frac{(-2+x)(-2+5x+x^2)H_{2,1,1}}{24(-1+x)^3}+\frac{(1+x)(-1+3x)H_{-1,0,1}}{(-1+x)x}-\frac{(1+17x-4x^2+2x^3)H_{0,0,0,1}}{4(-1+x)^3}\\
&-\frac{(3+11x+2x^2)H_{0,0,1,1}}{2(-1+x)^3}+\frac{1}{2}H_{1,1,0,1}+3H_{1,1,1,1}+\frac{(2+14x-x^2+x^3)H_{0,1,0,1}}{4(-1+x)^3}+\frac{3}{2}H_{0,1,1,1}-H_{0,-1,0,1}-H_{1,0,0,1}\Big\}\\
&+C_FT_Fn_h\Big\{\frac{2267-5398x+4283x^2}{1296(-1+x)^2}-\frac{\pi^2(-11+45x-57x^2+7x^3)}{108(-1+x)^3}+\frac{2(-6+13x-14x^2+19x^3)H_1}{27(-1+x)^2x}\\
&-\frac{(1+x)(-3+5x-5x^2+11x^3)H_{0,1}}{18(-1+x)^3x}+\frac{1}{6}H_{0,0,1}-\frac{\zeta_3}{6}\Big\}+C_FT_Fn_l\Big\{\frac{7859}{5184}+\frac{1}{864}\pi^2(109+48H_1)\\
&+\frac{(-12+31x)H_1}{27x}-\frac{(3-11x)H_{0,1}}{18x}-\frac{(3-11x)H_{1,1}}{9x}+\frac{1}{6}H_{0,0,1}+\frac{1}{3}H_{0,1,1}+\frac{1}{3}H_{1,0,1}+\frac{2}{3}H_{1,1,1}+\frac{13\zeta_3}{72}\Big\}. \qquad (31)
\end{aligned}
$$

The one-loop order has successfully been compared to Ref. [61] up to order ϵ^2 and has been extended to ϵ^4. Similarly, our two-loop results up to the constant part in ϵ agrees with Ref. [61] and we have added ϵ^1 and ϵ^2 terms.

After multiplying $\Gamma^t_{\mu\nu}(q_1,q_2)$ in Eq. (3) with q^ν and projecting the result to F_2^v we obtain the contribution for $b\to s\gamma$ which is given by

$$F_1^t-\frac{1}{2}F_2^t-\frac{1}{2}F_3^t. \qquad (32)$$

Using our analytic results we find agreement with the numerical expressions given in Eqs. (88) and (89) of Ref. [69].

At three-loop order the amplitude can be divided up into the different color factors[4]

$$
\begin{aligned}
F_i^{x,(3)} &= C_FT_F^2n_l^2F_i^{x,(3),n_l^2}+C_FT_F^2n_h^2F_i^{x,(3),n_h^2}+C_FT_F^2n_ln_hF_i^{x,(3),n_ln_h}+C_F^2T_Fn_lF_i^{x,(3),C_Fn_l}+C_FC_AT_Fn_lF_i^{x,(3),C_An_l}\\
&\quad+N_C^3F_i^{x,(3),N_C^3}+C_F^2n_hT_FF_i^{x,(3),C_Fn_h}+C_FC_An_hT_FF_i^{x,(3),C_An_h}+\mathcal{O}(N_C^2) \qquad (33)
\end{aligned}
$$

[4]The same color decomposition also holds for the infrared subtracted quantities C.

up to color suppressed contributions. We have computed the first six terms analytically. The corresponding expressions can again be downloaded from the webpage [164]. The explicit three-loop expressions for the tensor coefficient C_1^t read

$$\begin{aligned}C_1^{t,(3),n_l^2} =& -\frac{370949}{419904}-\frac{221\pi^4}{38880}-\pi^2\left(\frac{829}{3888}-\frac{(3-11x)H_1}{81x}+\frac{1}{27}H_{0,1}+\frac{2}{27}H_{1,1}\right)\\&+\frac{(657-1430x)H_1}{1458x}+\frac{(48-121x)H_{0,1}}{162x}+\frac{(48-121x)H_{1,1}}{81x}\\&+\frac{(3-11x)H_{0,0,1}}{27x}+\frac{2(3-11x)H_{0,1,1}}{27x}+\frac{2(3-11x)H_{1,0,1}}{27x}-\frac{4}{9}H_{1,1,0,1}\\&+\frac{4(3-11x)H_{1,1,1}}{27x}-\frac{1}{9}H_{0,0,0,1}-\frac{2}{9}H_{0,0,1,1}-\frac{2}{9}H_{0,1,0,1}-\frac{4}{9}H_{0,1,1,1}\\&-\frac{2}{9}H_{1,0,0,1}-\frac{4}{9}H_{1,0,1,1}-\frac{8}{9}H_{1,1,1,1}-\frac{(323+126H_1)\zeta_3}{486},\end{aligned}\tag{34}$$

$$\begin{aligned}C_1^{t,(3),n_h^2} =& -\frac{\pi^4}{540}+\frac{\pi^2(5+3x)}{135(1-x)}-\frac{667-2704x+4273x^2-3070x^3+810x^4}{324(1-x)^4}\\&+\zeta_3\left(\frac{21-162x+483x^2-668x^3+477x^4-198x^5+39x^6}{27(-1+x)^6}+\frac{2}{9}H_1\right)\\&+\frac{(438-2147x+4124x^2-4926x^3+3734x^4-1079x^5)H_1}{972(1-x)^4x}\\&+\frac{(1+x)(48-193x+282x^2-346x^3+354x^4-121x^5)H_{0,1}}{162(1-x)^5x}\\&+\frac{(3-11x+39x^2-123x^3+153x^4-75x^5+33x^6-11x^7)}{27(1-x)^6x}H_{0,0,1}\\&-\frac{1}{9}H_{0,0,0,1}-\frac{2}{9}H_{1,0,0,1},\end{aligned}\tag{35}$$

$$\begin{aligned}C_1^{t,(3),n_h n_l} =& -\frac{\pi^4}{810}-\frac{23611-43766x+9787x^2}{5832(1-x)^2}+\pi^2\left(\frac{371-585x-327x^2+349x^3}{1944(1-x)^3}\right.\\&\left.-\frac{(1+x)(3-5x+5x^2-11x^3)H_1}{81(1-x)^3x}+\frac{1}{27}H_{0,1}\right)+\frac{(73-308x+421x^2-138x^3)H_1}{81(1-x)^2x}-\frac{2}{9}H_{0,0,0,1}-\frac{2}{9}H_{0,0,1,1}\\&+\frac{(48-157x+153x^2-27x^3+31x^4)H_{0,1}}{81(1-x)^3x}+\frac{8(6-13x+14x^2-19x^3)H_{1,1}}{81(1-x)^2x}\\&+\frac{2(3-11x+27x^2-24x^3-11x^4)H_{0,0,1}}{27(1-x)^3x}+\frac{2(1+x)(3-5x+5x^2-11x^3)H_{0,1,1}}{27(1-x)^3x}-\frac{2}{9}H_{0,1,0,1}\\&+\frac{2(10-20x+x^2)\zeta_3}{27(1-x)^2}+\frac{2(1+x)(3-5x+5x^2-11x^3)H_{1,0,1}}{27(1-x)^3x},\end{aligned}\tag{36}$$

$$
\begin{aligned}
C_1^{t,(3),C_R n_l} = &-\frac{82223}{62208} + H_{0,-1,0,1,1} + \pi^4\left(\frac{52459 + 113919x - 71799x^2 + 48173x^3}{622080(-1+x)^3} + \frac{61H_1}{4320}\right) \\
&+ \zeta_3\left(-\frac{6142 - 6438x - 3345x^2 + 3155x^3}{2592(-1+x)^3}\right. \\
&- \frac{(-73 + 70x - 473x^2 + 284x^3)H_1}{144(-1+x)^2x} + \frac{7(-2+x)(-2+5x+x^2)H_2}{144(-1+x)^3} \\
&\left.- \frac{(1+x)(-1+3x)H_{-1}}{4(-1+x)x} - \frac{(-49 + 387x - 231x^2 + 85x^3)H_{0,1}}{144(-1+x)^3} + \frac{1}{4}H_{0,-1} - \frac{91}{72}H_{1,1}\right) \\
&+ \pi^2\left[\frac{575209 + 500974x + 5545x^2}{248832(-1+x)^2} + \ln(2)\left(\frac{280 - 516x + 249x^2 + 5x^3}{144(-1+x)^3} + \frac{(7+17x)H_1}{36(-1+x)} - \frac{1}{6}H_{0,-1} + \frac{1}{6}H_{1,1}\right.\right. \\
&\left. + \frac{(-2+x)(-2+5x+x^2)H_2}{72(-1+x)^3} + \frac{(1+x)(-1+3x)H_{-1}}{6(-1+x)x}\right) \\
&- \frac{(1569 - 14528x - 11363x^2 + 2434x^3)H_1}{5184(-1+x)^2x} + \frac{(2-x)(26 - 31x + 23x^2)H_2}{144(1-x)^3} \\
&- \frac{(1+x)(41 - 131x + 102x^2)H_{-1}}{216(-1+x)^2x} - \frac{(-402 + 2899x + 1347x^2 - 2175x^3 + 923x^4)H_{0,1}}{1728(-1+x)^3x} \\
&- \frac{(-12 + 71x - 117x^2 + 15x^3 + 19x^4)H_{0,-1}}{216(-1+x)^3x} - \frac{(90 - 1117x - 1636x^2 + 359x^3)H_{1,1}}{864(-1+x)^2x} \\
&+ \frac{(6+x)H_{1,2}}{36x} - \frac{(1+x)(-1+3x)H_{1,-1}}{18(-1+x)x} + \frac{(-2+x)(-2+5x+x^2)H_{2,1}}{72(-1+x)^3} - \frac{(-2+x)(-2+5x+x^2)H_{2,2}}{72(-1+x)^3} \\
&+ \frac{(1+x)(-1+3x)H_{-1,1}}{9(-1+x)x} + \frac{(1+x)(-1+3x)H_{-1,-1}}{18(-1+x)x} + \frac{(-107 - 79x - 181x^2 + 47x^3)H_{0,0,1}}{288(-1+x)^3} + \frac{1}{18}H_{0,0,-1} \\
&- \frac{(21 + 97x + 7x^2 + 3x^3)H_{0,1,1}}{48(-1+x)^3} - \frac{1}{6}H_{0,1,2} + \frac{1}{18}H_{0,1,-1} - \frac{1}{9}H_{0,-1,1} - \frac{1}{18}H_{0,-1,-1} \\
&- \frac{1}{144}H_{1,0,1} - \frac{13}{72}H_{1,1,1} - \frac{1}{6}H_{1,1,2} - \frac{(40 - 72x + 15x^2 + 13x^3)\ln^2(2)}{108(-1+x)^3} \\
&\left. + \frac{(725 + 14145x - 3537x^2 + 1723x^3)\zeta_3}{3456(-1+x)^3}\right] - \frac{(-7103 + 22516x)H_1}{10368x} \\
&+ \frac{(4608 - 27263x + 80878x^2 + 36529x^3)H_{0,1}}{10368(-1+x)^2x} + \frac{(-432 + 2976x + 44615x^2 + 217x^3)H_{1,1}}{5184(-1+x)x^2} \\
&+ \frac{(14 + 217x + 207x^2 - 730x^3 + 274x^4)H_{0,0,1}}{72(-1+x)^3x} - \frac{(246 - 3392x + 3372x^2 - 363x^3 + 83x^4)H_{0,1,1}}{216(-1+x)^3x} \\
&+ \frac{(-90 + 701x + 1220x^2 + 89x^3)H_{1,0,1}}{216(-1+x)^2x} - \frac{(18 - 87x + 19x^2)H_{1,1,1}}{9(-1+x)x} \\
&+ \frac{(-2+x)(26 - 31x + 23x^2)H_{2,1,1}}{72(-1+x)^3} - \frac{(1+x)(41 - 131x + 102x^2)H_{-1,0,1}}{18(-1+x)^2x} \\
&+ \frac{(12 + 22x + 338x^2 - 415x^3 + 127x^4)H_{0,0,0,1}}{36(-1+x)^3x} - \frac{(12 - 285x - 121x^2 + 128x^3 + 22x^4)H_{0,0,1,1}}{36(-1+x)^3x} \\
&- \frac{(-9 + 34x + 13x^2 + 25x^3 + x^4)H_{0,1,0,1}}{18(-1+x)^3x} - \frac{(21 - 231x + 339x^2 - 270x^3 + 137x^4)H_{0,1,1,1}}{18(-1+x)^3x} \\
&- \frac{(-12 + 71x - 117x^2 + 15x^3 + 19x^4)H_{0,-1,0,1}}{18(-1+x)^3x} + \frac{(-24 + 17x - 238x^2 + 101x^3)H_{1,0,0,1}}{36(-1+x)^2x}
\end{aligned}
$$

$$
\begin{aligned}
&-\frac{(-15+140x-109x^2+80x^3)H_{1,0,1,1}}{18(-1+x)^2x}-\frac{(-12-5x-254x^2+79x^3)H_{1,1,0,1}}{36(-1+x)^2x}-\frac{10(-1+3x)H_{1,1,1,1}}{3x}\\
&+\frac{(6+x)H_{1,2,1,1}}{18x}-\frac{2(1+x)(-1+3x)H_{1,-1,0,1}}{3(-1+x)x}+\frac{(-2+x)(-2+5x+x^2)H_{2,1,1,1}}{18(-1+x)^3}\\
&-\frac{(-2+x)(-2+5x+x^2)H_{2,2,1,1}}{36(-1+x)^3}-\frac{5(1+x)(-1+3x)H_{-1,0,0,1}}{6(-1+x)x}-\frac{(1+x)(-1+3x)H_{-1,0,1,1}}{(-1+x)x}\\
&-\frac{2(1+x)(-1+3x)H_{-1,1,0,1}}{3(-1+x)x}+\frac{2(1+x)(-1+3x)H_{-1,-1,0,1}}{3(-1+x)x}+\frac{(1+17x-4x^2+2x^3)H_{0,0,0,0,1}}{3(-1+x)^3}\\
&+\frac{(5+25x+x^2+x^3)H_{0,0,0,1,1}}{3(-1+x)^3}+\frac{(-4+32x-19x^2+7x^3)H_{0,0,1,0,1}}{12(-1+x)^3}-\frac{(1+x)(15+20x-3x^2)H_{0,0,1,1,1}}{6(1-x)^3}\\
&+\frac{2}{3}H_{0,0,-1,0,1}+\frac{(-2+66x-27x^2+11x^3)H_{0,1,0,0,1}}{12(-1+x)^3}-\frac{(-9-13x-13x^2+3x^3)H_{0,1,0,1,1}}{6(-1+x)^3}\\
&-\frac{(1+17x-4x^2+2x^3)H_{0,1,1,0,1}}{3(-1+x)^3}-\frac{10}{3}H_{0,1,1,1,1,1}-\frac{1}{3}H_{0,1,2,1,1}+\frac{2}{3}H_{0,1,-1,0,1}+\frac{5}{6}H_{0,-1,0,0,1}\\
&+\frac{2}{3}H_{0,-1,1,0,1}-\frac{2}{3}H_{0,-1,-1,0,1}+2H_{1,0,0,0,1}+\frac{2}{3}H_{1,0,1,0,1}-3H_{1,0,1,1,1}+\frac{11}{6}H_{1,1,0,0,1}-2H_{1,1,0,1,1}\\
&-\frac{4}{3}H_{1,1,1,0,1}-\frac{20}{3}H_{1,1,1,1,1,1}-\frac{1}{3}H_{1,1,2,1,1}-\frac{(68-108x+21x^2+23x^3)\ln^4(2)}{432(-1+x)^3}-\frac{(68-108x+21x^2+23x^3)\mathrm{Li}_4(\frac{1}{2})}{18(-1+x)^3}\\
&+\frac{(-13-21x-18x^2+4x^3)\zeta_5}{9(-1+x)^3},
\end{aligned}
\tag{37}
$$

$$
\begin{aligned}
C_1^{t,(3),C_An_l}=&\frac{4126157}{419904}+\pi^4\left(-\frac{113-9573x-7707x^2+2935x^3}{155520(-1+x)^3}-\frac{19}{864}H_1\right)+\zeta_3\left(\frac{-5092+21000x-29703x^2+13309x^3}{5184(-1+x)^3}\right.\\
&-\frac{1}{8}H_{0,-1}+\frac{3}{8}H_{1,1}+\frac{(-36+113x-202x^2+173x^3)H_1}{144(-1+x)^2x}-\frac{7(-2+x)(-2+5x+x^2)H_2}{288(-1+x)^3}\\
&\left.+\frac{(1+x)(-1+3x)H_{-1}}{8(-1+x)x}+\frac{(-7+17x-24x^2+6x^3)H_{0,1}}{24(-1+x)^3}\right)\\
&+\pi^2\left[\frac{236191-273122x+373243x^2}{279936(-1+x)^2}+\ln(2)\left(-\frac{280-516x+249x^2+5x^3}{288(-1+x)^3}-\frac{(7+17x)H_1}{72(-1+x)}\right.\right.\\
&\left.-\frac{(-2+x)(-2+5x+x^2)H_2}{144(-1+x)^3}-\frac{(1+x)(-1+3x)H_{-1}}{12(-1+x)x}+\frac{1}{12}H_{0,-1}-\frac{1}{12}H_{1,1}\right)\\
&+\frac{(-108+8077x-5921x^2+7780x^3)H_1}{7776(-1+x)^2x}-\frac{(-2+x)(26-31x+23x^2)H_2}{288(-1+x)^3}\\
&+\frac{(1+x)(41-131x+102x^2)H_{-1}}{432(-1+x)^2x}+\frac{(-16+4x-110x^2-145x^3+87x^4)H_{0,1}}{288(-1+x)^3x}\\
&+\frac{(-12+71x-117x^2+15x^3+19x^4)H_{0,-1}}{432(-1+x)^3x}+\frac{(96+71x+74x^2+335x^3)H_{1,1}}{864(-1+x)^2x}-\frac{(6+x)H_{1,2}}{72x}\\
&+\frac{(1+x)(-1+3x)H_{1,-1}}{36(-1+x)x}-\frac{(-2+x)(-2+5x+x^2)H_{2,1}}{144(-1+x)^3}+\frac{(-2+x)(-2+5x+x^2)H_{2,2}}{144(-1+x)^3}\\
&-\frac{(1+x)(-1+3x)H_{-1,1}}{18(-1+x)x}-\frac{(1+x)(-1+3x)H_{-1,-1}}{36(-1+x)x}-\frac{(-3+29x+6x^2+8x^3)H_{0,0,1}}{144(-1+x)^3}\\
&-\frac{1}{36}H_{0,0,-1}+\frac{1}{12}H_{0,1,2}-\frac{1}{36}H_{0,1,-1}-\frac{(-1+15x+6x^2+4x^3)H_{0,1,1}}{36(-1+x)^3}+\frac{1}{36}H_{0,-1,-1}+\frac{1}{18}H_{0,-1,1}
\end{aligned}
$$

$$
\begin{aligned}
&-\frac{1}{9}H_{1,1,1}+\frac{1}{12}H_{1,1,2}-\frac{(40-72x+15x^2+13x^3)\ln^2(2)}{216(1-x)^3}-\frac{(53-23x+261x^2-19x^3)\zeta_3}{288(1-x)^3}\Bigg]\\
&+\frac{(-98586+201431x)H_1}{23328x}+\frac{(-2742+10661x-10999x^2+5906x^3)H_{0,1}}{1296(-1+x)^2x}+\frac{(4431-14722x+13117x^2)H_{1,1}}{1296(-1+x)x}\\
&+\frac{(264-968x+2619x^2-2079x^3+218x^4)H_{0,0,1}}{432(-1+x)^3x}+\frac{(420-2539x+7119x^2-7008x^3+1954x^4)H_{0,1,1}}{432(-1+x)^3x}\\
&+\frac{(-501+3274x-3920x^2+2143x^3)H_{1,0,1}}{432(-1+x)^2x}+\frac{(393-2044x+1915x^2)H_{1,1,1}}{216(-1+x)x}\\
&-\frac{(-2+x)(26-31x+23x^2)H_{2,1,1}}{144(-1+x)^3}+\frac{(1+x)(41-131x+102x^2)H_{-1,0,1}}{36(-1+x)^2x}-\frac{(40+170x+177x^2-159x^3)H_{0,0,0,1}}{144(1-x)^3}\\
&+\frac{(2+163x-99x^2+10x^3)H_{0,0,1,1}}{36(-1+x)^3}+\frac{(-145+325x-414x^2+94x^3)H_{0,1,0,1}}{144(-1+x)^3}\\
&+\frac{(-125+651x-753x^2+219x^3)H_{0,1,1,1}}{72(-1+x)^3}+\frac{(-12+71x-117x^2+15x^3+19x^4)H_{0,-1,0,1}}{36(-1+x)^3x}\\
&-\frac{(-3+x+10x^2+10x^3)H_{1,0,0,1}}{18(-1+x)^2x}+\frac{(38-109x+47x^2)H_{1,0,1,1}}{18(-1+x)^2}+\frac{(377-586x+401x^2)H_{1,1,0,1}}{144(-1+x)^2}\\
&+\frac{44}{9}H_{1,1,1,1}-\frac{(6+x)H_{1,2,1,1}}{36x}+\frac{(1+x)(-1+3x)H_{1,-1,0,1}}{3(-1+x)x}-\frac{(-2+x)(-2+5x+x^2)H_{2,1,1,1}}{36(-1+x)^3}\\
&+\frac{(-2+x)(-2+5x+x^2)H_{2,2,1,1}}{72(-1+x)^3}+\frac{5(1+x)(-1+3x)H_{-1,0,0,1}}{12(-1+x)x}+\frac{(1+x)(-1+3x)H_{-1,0,1,1}}{2(-1+x)x}\\
&+\frac{(1+x)(-1+3x)H_{-1,1,0,1}}{3(-1+x)x}-\frac{(1+x)(-1+3x)H_{-1,-1,0,1}}{3(-1+x)x}+\frac{(1+x+6x^2)H_{0,0,0,0,1}}{6(-1+x)^3}\\
&+\frac{(1+x+6x^2)H_{0,0,0,1,1}}{3(-1+x)^3}+\frac{(1+x+6x^2)H_{0,0,1,0,1}}{24(-1+x)^3}+\frac{(1+x+6x^2)H_{0,0,1,1,1}}{3(-1+x)^3}-\frac{1}{3}H_{0,0,-1,0,1}\\
&-\frac{(-7+9x-30x^2+4x^3)H_{0,1,0,0,1}}{24(-1+x)^3}+\frac{(1+x+6x^2)H_{0,1,0,1,1}}{6(-1+x)^3}-\frac{(1+x+6x^2)H_{0,1,1,0,1}}{6(-1+x)^3}\\
&+\frac{1}{6}H_{0,1,2,1,1}-\frac{1}{3}H_{0,1,-1,0,1}-\frac{5}{12}H_{0,-1,0,0,1}-\frac{1}{2}H_{0,-1,0,1,1}-\frac{1}{3}H_{0,-1,1,0,1}+\frac{1}{3}H_{0,-1,-1,0,1}-\frac{11}{12}H_{1,0,0,0,1}\\
&-\frac{2}{3}H_{1,0,0,1,1}-\frac{1}{3}H_{1,0,1,0,1}-H_{1,1,0,0,1}-\frac{1}{6}H_{1,1,0,1,1}+\frac{1}{6}H_{1,1,2,1,1}+\frac{(68-108x+21x^2+23x^3)\ln^4(2)}{864(-1+x)^3}\\
&+\frac{(68-108x+21x^2+23x^3)\mathrm{Li}_4(\frac{1}{2})}{36(-1+x)^3}-\frac{(-43+161x-105x^2+51x^3)\zeta_5}{48(-1+x)^3},
\end{aligned}
\tag{38}
$$

$$
\begin{aligned}
C_1^{t,(3),N_c^3}=&-\frac{155263507}{26873856}-\frac{\pi^6(-7514867-19812135x-18106521x^2+692147x^3)}{1672151040(-1+x)^3}\\
&+\zeta_5\left(\frac{1199+6609x+3760x^2+162x^3}{768(-1+x)^3}-\frac{(-18-12x-43x^2+7x^3)H_1}{16(-1+x)^3}\right)\\
&+\pi^4\left(-\frac{347993+1668009x-548373x^2+39943x^3}{4976640(-1+x)^3}+\frac{(555-14839x+13219x^2+18643x^3+8342x^4)H_1}{368640(-1+x)^3x}\right.\\
&\left.-\frac{(2691+21975x+7817x^2+2749x^3)H_{0,1}}{368640(-1+x)^3}-\frac{(-3053-1209x-7431x^2+1325x^3)H_{1,1}}{184320(-1+x)^3}\right)
\end{aligned}
$$

$$
\begin{aligned}
&+\zeta_3\left(\frac{41639-91621x+51926x^2}{62208(-1+x)^2}-\frac{(570-7411x+3221x^2-4264x^3)H_1}{3456(1-x)^2x}\right.\\
&+\frac{(-18-703x-1779x^2-2751x^3+139x^4)H_{0,1}}{1152(-1+x)^3x}-\frac{15}{32}H_{1,1,1}+\frac{(90+118x-479x^2+325x^3)H_{1,1}}{576(-1+x)^2x}\\
&\left.+\frac{(-1+2x)(1+8x)H_{0,0,1}}{32(-1+x)^3}-\frac{(-5+15x-12x^2+5x^3)H_{0,1,1}}{32(-1+x)^3}-\frac{(7+123x-3x^2+17x^3)H_{1,0,1}}{64(-1+x)^3}\right)\\
&+\pi^2\left[-\frac{100078387+125792410x+60503731x^2}{71663616(-1+x)^2}-\frac{17}{128}H_{1,1,1,1}-\zeta_3\left(\frac{6599+36435x+8073x^2+4549x^3}{27648(-1+x)^3}\right.\right.\\
&\left.+\frac{(335+147x+813x^2-143x^3)H_1}{4608(1-x)^3}\right)-\frac{(-43983+479108x+357953x^2+115742x^3)H_1}{248832(-1+x)^2x}\\
&+\frac{(-1028+5603x+12013x^2+1157x^3+867x^4)H_{0,1}}{9216(-1+x)^3x}+\frac{(1569-1715x-12797x^2+307x^3)H_{1,1}}{13824(-1+x)^2x}\\
&-\frac{(177+146x+2244x^2-1034x^3+27x^4)H_{0,0,1}}{4608(-1+x)^3x}+\frac{(-270-1433x+5199x^2+2331x^3+689x^4)H_{0,1,1}}{4608(-1+x)^3x}\\
&+\frac{(-192-295x-1719x^2-21x^3+67x^4)H_{1,0,1}}{4608(-1+x)^3x}+\frac{(117+1106x+893x^2+476x^3)H_{1,1,1}}{2304(-1+x)^2x}\\
&+\frac{(59+423x+23x^2+23x^3)H_{0,0,0,1}}{768(1-x)^3}-\frac{(9+45x+7x^2+2x^3)H_{0,0,1,1}}{64(-1+x)^3}-\frac{(59+447x+109x^2+33x^3)H_{0,1,0,1}}{1536(-1+x)^3}\\
&-\frac{(23+219x+21x^2+25x^3)H_{0,1,1,1}}{256(-1+x)^3}-\frac{(1+9x+x^2+x^3)H_{1,0,0,1}}{32(-1+x)^3}-\frac{(19+183x+17x^2+21x^3)H_{1,0,1,1}}{384(-1+x)^3}\\
&\left.-\frac{(23+219x+21x^2+25x^3)H_{1,1,0,1}}{768(-1+x)^3}\right]-\frac{(-8459523+13259174x)H_1}{2985984x}-\frac{(7125-3574x-11219x^2)H_{1,1,1}}{3456(1-x)x}\\
&-\frac{(-422544+762395x+879722x^2+1494251x^3)H_{0,1}}{331776(-1+x)^2x}-\frac{(-7560+266112x+108349x^2+990011x^3)H_{1,1}}{165888(-1+x)x^2}\\
&-\frac{(-4440-16709x-45452x^2+10171x^3)H_{0,0,1}}{6912(-1+x)^2x}-\frac{(18+930x-8811x^2-8782x^3+2299x^4)H_{0,1,1}}{1152(-1+x)^2x^2}\\
&-\frac{(54-5736x+38353x^2-10940x^3+23143x^4)H_{1,0,1}}{6912(-1+x)^2x^2}-\frac{(420+3485x+13593x^2-9713x^3+1521x^4)H_{0,0,0,1}}{2304(-1+x)^3x}\\
&+\frac{(366-1722x-4797x^2+1084x^3+416x^4)H_{0,0,1,1}}{576(-1+x)^3x}-\frac{(450-2581x+1089x^2-8599x^3+335x^4)H_{0,1,0,1}}{2304(-1+x)^3x}\\
&+\frac{(-1752+1163x+5102x^2+3191x^3)H_{0,1,1,1}}{1152(-1+x)^2x}-\frac{(-93-934x-4054x^2+545x^3)H_{1,0,0,1}}{1152(-1+x)^2x}\\
&+\frac{(-101+323x+42x^2+216x^3)H_{1,0,1,1}}{192(-1+x)^2x}-\frac{(-186+227x-700x^2+677x^3)H_{1,1,0,1}}{1152(-1+x)^2x}\\
&+\frac{(249-98x+497x^2)H_{1,1,1,1}}{144(-1+x)x}-\frac{(12+233x+1137x^2-400x^3+104x^4)H_{0,0,0,0,1}}{384(-1+x)^3x}\\
&-\frac{(-60-163x-423x^2+158x^3+26x^4)H_{0,0,0,1,1}}{192(-1+x)^3x}-\frac{(6+6x+570x^2-77x^3+47x^4)H_{0,0,1,0,1}}{192(-1+x)^3x}\\
&+\frac{(15+379x-21x^2-622x^3+3x^4)H_{0,0,1,1,1}}{96(-1+x)^3x}-\frac{(-6+79x+723x^2+33x^3+53x^4)H_{0,1,0,0,1}}{192(-1+x)^3x}\\
&+\frac{(24+13x+375x^2-379x^3+27x^4)H_{0,1,0,1,1}}{192(-1+x)^3x}+\frac{(-12-517x+495x^2-82x^3+122x^4)H_{0,1,1,0,1}}{384(-1+x)^3x}
\end{aligned}
$$

$$
\begin{aligned}
&+\frac{(18-133x-364x^2+47x^3)H_{0,1,1,1,1,1}}{48(-1+x)^2x}+\frac{(9+x+3x^2+165x^3+2x^4)H_{1,0,0,0,1}}{192(-1+x)^3x}\\
&+\frac{(18-148x+309x^2-90x^3+91x^4)H_{1,0,0,1,1}}{96(-1+x)^3x}+\frac{(4+9x+42x^2+9x^3-4x^4)H_{1,0,1,0,1}}{64(1-x)^3x}\\
&+\frac{(1+5x)(4-10x+5x^2)H_{1,0,1,1,1}}{16(1-x)^2x}-\frac{(6+29x+107x^2-16x^3)H_{1,1,0,0,1}}{192(1-x)^2x}\\
&+\frac{(6+160x-155x^2+115x^3)H_{1,1,0,1,1}}{96(1-x)^2x}+\frac{(151-14x+79x^2)H_{1,1,1,0,1}}{96(-1+x)^2}+\frac{5(9+26x)H_{1,1,1,1,1}}{48x}\\
&-\frac{(2+24x+15x^2+4x^3)H_{0,0,0,0,0,0,1}}{32(-1+x)^3}+\frac{(7+57x-3x^2+5x^3)H_{0,0,0,0,1,1}}{16(-1+x)^3}-\frac{(5+36x+2x^2+2x^3)H_{0,0,0,1,0,1}}{32(-1+x)^3}\\
&+\frac{(23+99x+29x^2+5x^3)H_{0,0,0,1,1,1}}{16(-1+x)^3}-\frac{(1+12x+6x^2+2x^3)H_{0,0,1,0,0,1}}{32(-1+x)^3}+\frac{(4+33x+2x^2+3x^3)H_{0,0,1,0,1,1}}{16(-1+x)^3}\\
&-\frac{(14+48x+7x^2)H_{0,0,1,1,0,1}}{32(-1+x)^3}+\frac{3(1+x)(1+2x)H_{0,0,1,1,1,1}}{2(-1+x)^3}-\frac{x(3+5x+x^2)H_{0,1,0,0,0,1}}{32(-1+x)^3}\\
&-\frac{3(1+2x+3x^2)H_{0,1,0,0,1,1}}{16(-1+x)^3}-\frac{(5+27x+15x^2+x^3)H_{0,1,0,1,0,1}}{64(-1+x)^3}-\frac{(-11+9x-17x^2+7x^3)H_{0,1,0,1,1,1}}{32(-1+x)^3}\\
&+\frac{(2+18x-x^2+2x^3)H_{0,1,1,0,0,1}}{32(-1+x)^3}-\frac{(2+18x-x^2+2x^3)H_{0,1,1,0,1,1}}{16(-1+x)^3}-\frac{3(3+15x+5x^2+x^3)H_{0,1,1,1,0,1}}{32(-1+x)^3}\\
&+\frac{(1+9x+x^2+x^3)H_{1,0,0,0,0,1}}{16(-1+x)^3}+\frac{3(1+9x+x^2+x^3)H_{1,0,0,0,1,1}}{8(-1+x)^3}+\frac{3(1+x)(1+2x)H_{1,0,0,1,1,1}}{4(-1+x)^3}\\
&+\frac{(3+15x+5x^2+x^3)H_{1,0,1,0,1,1}}{16(-1+x)^3}-\frac{(2+12x+3x^2+x^3)H_{1,0,1,1,0,1}}{8(-1+x)^3}-\frac{3}{4}H_{1,0,1,1,1,1}+\frac{(1+9x+x^2+x^3)H_{1,1,0,0,0,1}}{16(-1+x)^3}\\
&+\frac{(1+x)(1+2x)H_{1,1,0,0,1,1}}{4(-1+x)^3}-\frac{(3+15x+5x^2+x^3)H_{1,1,0,1,0,1}}{32(-1+x)^3}-\frac{9}{16}H_{1,1,0,1,1,1}-\frac{3}{8}H_{1,1,1,0,1,1}-\frac{3}{16}H_{1,1,1,1,0,1}\\
&-\frac{15}{8}H_{1,1,1,1,1,1}-\frac{15}{16}H_{0,1,1,1,1,1}-\frac{(10+1185x-42x^2+197x^3)\zeta_3^2}{576(-1+x)^3},
\end{aligned}
\tag{39}
$$

where ζ_i denote the Riemann ζ function at integer argument i. Furthermore, we use the following convention for the iterated integrals:

$$H_{i,\vec{w}}(x)=\int_0^x \mathrm{d}t w_i(t)H_{\vec{w}}(t), \tag{40}$$

with the letters

$$w_0(t)=\frac{1}{t},\qquad w_{-1}(t)=\frac{1}{1+t},$$
$$w_1(t)=\frac{1}{1-t},\qquad w_2(t)=\frac{1}{2-t},$$

and we drop the argument for brevity, i.e. $H_{\vec{w}}(x)\equiv H_{\vec{w}}$. The first three letters define the harmonic polylogarithms. The forth letter can be avoided by allowing for harmonic polylogarithms evaluated at argument $1-x$.

We compared our analytic results for F_1^v, F_2^v, F_3^v, and F^s to the ones attached to Ref. [53] including ϵ^4 and ϵ^2 terms at one- and two-loop order, respectively. We found full agreement after adjusting for the different tensor basis and renormaliztion and after adapting the large-N_C limit and setting all fermionic contributions to zero.

V. NUMERICAL RESULTS

As mentioned in Sec. III C we compute all master integrals using the method "expand and match." As a result we obtain analytic expansions of the (unknown) three-loop expressions around the values s/m^2 given in Eq. (30) with high-precision numerical coefficients. Note that our approach provides generalized expansions which may contain logarithms of square roots of the expansion parameter, depending on the physical situation at the expansion point.

To illustrate the structure of our results we show in the following the first three expansion terms for $s/m^2 \to 1$ of the C_F^3 color factor of the renormalized and infrared subtracted form factor C_1^t. It is given by[5]

$$\begin{aligned} C_1^{t,(3)}|_{C_F^3} &= 3.95625 + 1.23578L_\beta - 1.02622L_\beta^2 + 1.06563L_\beta^3 - 0.37851L_\beta^4 + 0.0625L_\beta^5 - 0.0208333L_\beta^6 \\ &+ \beta(8.31567 + 3.58274L_\beta - 2.03938L_\beta^2 - 0.0683922L_\beta^3 - 0.4375L_\beta^4 + 0.125L_\beta^5) \\ &+ \beta^2(-3.51595 - 19.1367L_\beta + 4.25689L_\beta^2 + 1.3063L_\beta^3 + 0.614583L_\beta^4 - 0.1875L_\beta^5) \\ &+ \beta^3(9.9209 + 35.8225L_\beta - 2.05302L_\beta^2 - 4.15664L_\beta^3 + 0.194444L_\beta^4 + 0.125L_\beta^5) + O(\beta^4), \end{aligned} \tag{41}$$

where $\beta = (1 - m^2/s)/(1 + m^2/s)$ and $L_\beta = \log(-2\beta)$. One observes that the expansion is logarithmically divergent in the limit $\beta \to 0$, however, it does not contain power suppressed terms like $1/\beta^n$, which are present in the bare amplitude. Similarly, we have a power-log expansion around $s/m^2 = -\infty$. The expansion around the other s/m^2 values are all simple Taylor expansions.

We implement the expansions around the s/m^2 values of Eq. (30) in a Fortran program FFh2l which can be obtained from the website [55]. It is either possible to access the three-loop expressions within Fortran or via a *Mathematica* interface which has the same functionality. FFh2l provides results for the pole parts and finite contributions of all twelve ultraviolet renormalized form factors but also for the finite parts of the infrared subtracted form factors C. In the region

$$-75 < s/m^2 < 15/16 \tag{42}$$

we provide a grid by numerically evaluating our Taylor expansions and the analytic counterterms with the help of GiNaC [165,166]. Around the singular points $s/m^2 \to -\infty$ and $s/m^2 = 1$ we switch to dedicated power-log expansions as shown in Eq. (41). This includes expansions of the counterterms to increase stability. A more detailed description of FFh2l can be found in Appendix B.

As reference, we show in Fig. 2 the (finite) vector, scalar, and tensor form factors for $\mu^2 = m^2$ as a function of s/m^2 for $0 < s < m^2$. We remind the reader that the axialvector and pseudoscalar form factors are related to the vector form factors through Eq. (6) and that $C_3^t = C_4^t = 0$ as discussed in Sec. II D. For the color factor we have chosen $C_A = 3$, $C_F = 4/3$, and $T_F = 1/2$. Furthermore, we have $n_l = 4$ and $n_h = 1$. For the x axis we have chosen a logarithmic scale since there is only a mild variation of the from factors for $s \approx 0$. On the other hand, at all loop orders we observe Coulomb-like singularities close to threshold. It is straightforward to reproduce these plots by either using the analytic one- and two-loop expressions provided as an ancillary file or with the help of the package FFh2l.

[5]We truncate the numerical values to six significant digits and suppress trailing zeros.

There are several checks on the correctness of our calculation. First of all, we observe that the gauge parameter cancels in the ultraviolet renormalized expressions. The analytic contributions induced by the one- and two-loop results cancel against the numerical results from the bare three-loop form factors. We observe that this cancellation happens at the level of 10^{-23} or significantly better which at the same time is an indication for the precision of our semianalytic three-loop result.

An important check is the cancellation of the $1/\epsilon$ poles in the construction of C. As expected, there are poles up to $1/\epsilon^6$. All of them cancel after ultraviolet renormalization and infrared subtraction. Here, we proceed as in Refs. [39,40] and define

$$\delta(C^{(3)}|_{\epsilon^i}) = \frac{F^{(3)}|_{\epsilon^i} + F^{(\mathrm{CT}+Z)}|_{\epsilon^i}}{F^{(\mathrm{CT}+Z)}|_{\epsilon^i}}, \tag{43}$$

where $F^{(3)}$ stands for the bare three-loop contribution and $F^{(\mathrm{CT}+Z)}$ contains the contributions induced from the analytic tree-level, one- and two-loop terms due to ultraviolet renormalization ("CT"), and infrared subtraction ("Z"). In the region given by Eq. (42), we observe that there is a cancellation of at least 16 digits for each individual color of each form factor and each ϵ pole. Only for $s/m^2 > 15/16$ the cancellation of the grid drops below that due to the Coulomb-like singularity which supports our decision to switch to a dedicated expansion. In most parts of the phase space the cancellation is many orders of magnitude better as can be seen in Fig. 3 where we show the two worst cases of all form factors.

Remarkably, all six orders of ϵ cancel with a similar precision. Only a careful analysis reveals a slight trend towards worse precision for the lower poles. Especially in the region $0 < s/m^2 < 1$ the loss of precision when switching to the next expansion point is clearly visible, but remains on a very high level. On the negative axis, the precision curve is much smoother and only the matching from our boundary conditions at $s/m^2 = 0$ to $s/m^2 = -1/2$ and the matching from $s/m^2 = -60$ to $s/m^2 \to -\infty$ stick out.

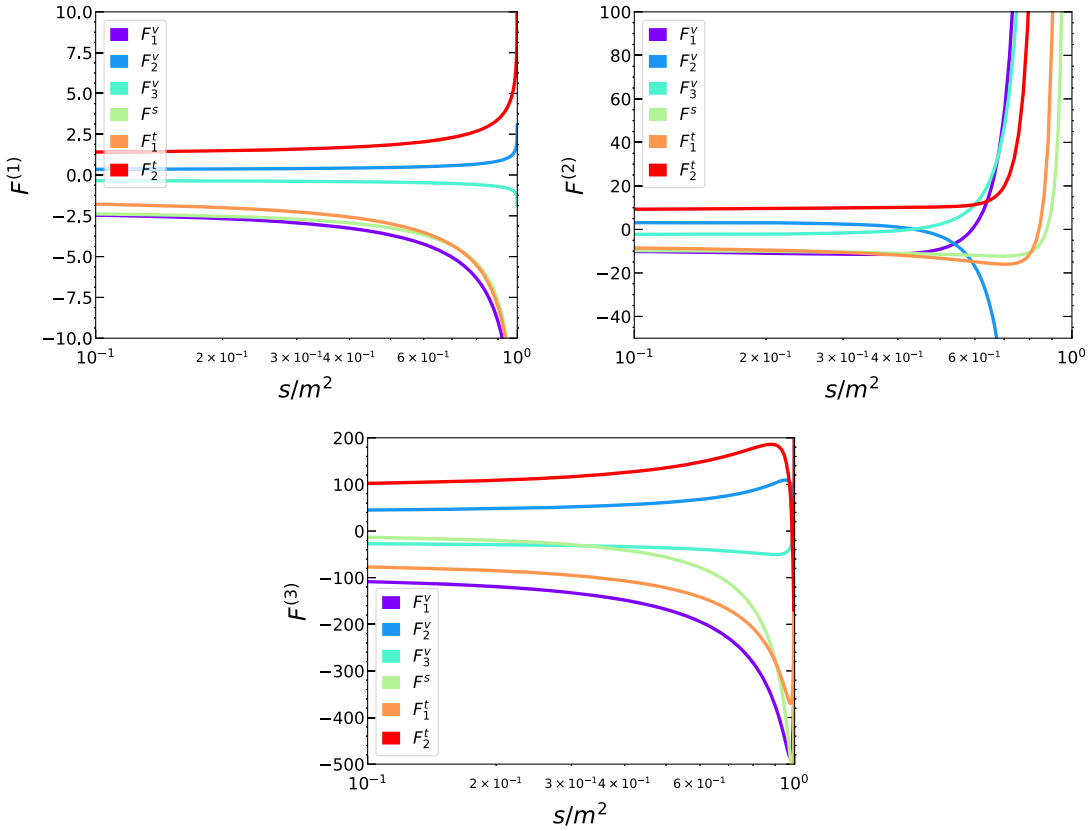

FIG. 2. One-, two-, and three-loop form factors as a function of s/m^2 for $s > 0$. The color factors have been adjusted to QCD with $n_l = 4$ and $n_h = 1$. For the renormalization scale $\mu^2 = m^2$ has been chosen.

Finally, we can also check the Ward identity from Eq. (11). Naively, one would expect that it allows us to estimate the precision of the finite terms similar to the pole cancellation. However, this is not the case. It was noticed in the two-loop calculation of Ref. [43] that the Ward identity is fulfilled already on the level of the master integrals. We observe something similar: the sum of the bare three-loop contributions and the sum of the counterterm contributions to Eq. (11) are separately constant, but nonzero, and vanish when summing both contributions. This suggests that there is a similar relation between the master integrals also at the three-loop level. Since in our calculation we do not express the renormalization constants in terms of master integrals, we check Eq. (11) only numerically and observe that it is fulfilled to high precision. In most parts of the phase space it exceeds our internal precision of 50 digits and only rarely drops below that at less stable points. Even at $s/m^2 \approx 0.9374$, where we switch to the dedicated power-log expansion due to the Coulomb-like singularity at the threshold, the Ward identity holds to at least 19 digits.

After all these considerations, we estimate the precision of the finite terms by extrapolating the pole cancellations and expect that our result is correct to at least 14 digits in the grid region given by Eq. (42) and usually many more in most parts of the phase space.

For the two singular power-log expansions around $s/m^2 \to -\infty$ and $s/m^2 = 1$ our strategy to estimate their precision differs slightly. As mentioned before, here we also expand the counterterms to increase stability. Hence, we can check the cancellation of the $1/\epsilon$ poles order by order in the expansion parameters $-m^2/s$ and $(1 - s/m^2)$, respectively. For the expansion around $s/m^2 \to -\infty$, we observe that they cancel with at least 15 digits up to order $(-m^2/s)^5$ and with at least 10 digits up to $(-m^2/s)^{17}$. The expansion around $s/m^2 = 1$ behaves worse and the coefficients cancel with at least 17 digits up to order $(1 - s/m^2)^1$, with at least ten digits up to $(1 - s/m^2)^3$, and with at least nine digits up to $(1 - s/m^2)^{20}$. Similarly, we can also check the Ward identity (11) order by order in the expansion parameters. Again we observe that it holds with high precision, reaching our internal precision of 50 digits for most expansion orders. Hence, we conservatively estimate that the two power-log expansions in the singular regions are sufficient to provide ten correct digits for the finite part.

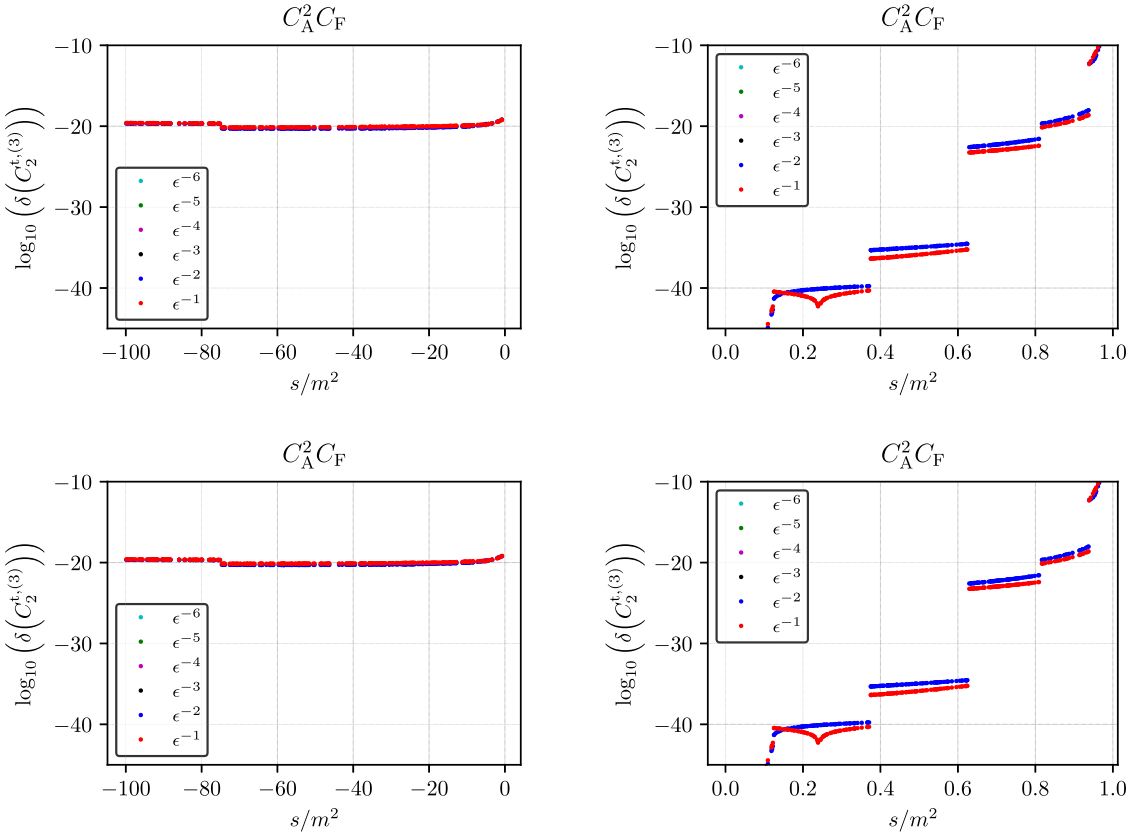

FIG. 3. Relative cancellation of the poles for the $C_A^2 C_F$ color structures of $C_1^{v,(3)}$ and $C_2^{t,(3)}$. They show the worst behavior of all form factors. The left panels cover the region $[-\infty, 0]$ and on the right results for $0 < s < 1$ are shown.

With this in mind, the grids and expansions provided in FFh2l are designed to provide at least ten correct digits over the full range $-\infty < s/m^2 < 1$.

VI. THE HARD FUNCTION IN $\bar{B} \to X_s\gamma$

In a SCET-based approach to $\bar{B} \to X_s\gamma$ the decay width is written as the product of a hard function with a convolution of the jet and soft function [62–64]. While the latter two are known to three loops already [65–68] the hard function was up to now only known to two loops [69–71]. With the three-loop matching coefficients of the tensor current at hand, we are now in the position to extract the hard function of $\bar{B} \to X_s\gamma$ to three loops as well.

To this end, we follow the discussions in Refs. [69–71] and consider the operator

$$Q_7 = -\frac{e\bar{m}_b(\mu)}{4\pi^2}(\bar{s}_L \sigma_{\mu\nu} F^{\mu\nu} b_R), \tag{44}$$

where $\bar{m}_b(\mu)$ is the bottom-quark mass in the $\overline{\text{MS}}$ scheme and e the electric charge of the positron. At leading power this operator is matched onto the SCET current

$$J^A = (\bar{\xi} W_{hc}) \not{\epsilon}_\perp (1-\gamma_5) h_v, \tag{45}$$

with the heavy quark effective theory (HQET) field h_v of the heavy quark, the SCET field ξ of the light quark, the hard-collinear Wilson line W_{hc}, and the polarization vector $\epsilon_\perp^\mu$ of the on-shell photon. The field strength tensor $F^{\mu\nu}$ in Eq. (44) gives rise to the Feynman rule

$$F^{\mu\nu} = \partial^\mu A^\nu - \partial^\nu A^\mu \longrightarrow i(q^\mu \epsilon_\perp^\nu - q^\nu \epsilon_\perp^\mu). \tag{46}$$

If the matching is done on shell, one can use $\epsilon_\perp \cdot q_2 = \epsilon_\perp \cdot q_1 = 0$, and arrive for $q^2 = 0$ at

$$\langle s\gamma | Q_7 | b \rangle = -\frac{e\bar{m}_b 2E_\gamma}{4\pi^2}\left(F_1^t - \frac{1}{2}F_2^t - \frac{1}{2}F_3^t\right)_{|q^2=0} \times J^A, \tag{47}$$

where $2E_\gamma \approx m_b$ at leading power. After infrared subtraction the expression in parenthesis becomes

$$C_\gamma \equiv C_1^t(s=0) - \frac{1}{2}C_2^t(s=0). \tag{48}$$

The factorization formula of $\bar{B} \to X_s\gamma$ is formulated on the level of the decay rate. Moreover, since the hard function $h_s(\mu)$ in $\bar{B} \to X_s\gamma$ is a genuine SCET object, the logarithms of the QCD scale ν have to be set to zero in the following. We therefore arrive at

$$h_s(\mu) = |C_{\gamma|L_\nu=0}|^2. \tag{49}$$

The explicit result of $h_s(\mu)$ to three loops reads

$$\begin{aligned}
h_s(\mu) = 1 &+ C_F\left[-L_\mu^2 - 5L_\mu - \frac{\pi^2}{6} - 12\right]\left(\frac{\alpha_s^{(n_l)}(\mu)}{4\pi}\right) + \left[\frac{1}{2}C_F^2L_\mu^4 + L_\mu^3\left(-\frac{11}{9}C_AC_F + 5C_F^2 + \frac{4}{9}C_Fn_lT_F\right)\right. \\
&+ \left(\left(\frac{\pi^2}{3} - \frac{299}{18}\right)C_AC_F + \left(\frac{49}{2} + \frac{\pi^2}{6}\right)C_F^2 + \frac{50}{9}C_Fn_lT_F\right)L_\mu^2 + \left(C_AC_F\left(22\zeta_3 - \frac{3925}{54} - \frac{16\pi^2}{9}\right)\right. \\
&+ C_F^2\left(-24\zeta_3 + \frac{117}{2} + \frac{17\pi^2}{6}\right) + \left(\frac{682}{27} + \frac{8\pi^2}{9}\right)C_Fn_lT_F\Big)L_\mu + C_FT_F\left(\frac{7126}{81} - \frac{16\zeta_3}{3} - \frac{232\pi^2}{27}\right) \\
&+ C_AC_F\left(-\frac{122443}{648} + \frac{478\zeta_3}{9} + \frac{829\pi^2}{108} + \frac{31\pi^4}{60} - \frac{74}{3}\pi^2\ln(2)\right) + C_F^2\left(\frac{3379}{24} - 88\zeta_3 - 25\pi^2 - \frac{47\pi^4}{72} + \frac{148}{3}\pi^2\ln(2)\right) \\
&\left.+ C_Fn_lT_F\left(\frac{52\zeta_3}{9} + \frac{7859}{162} + \frac{109\pi^2}{27}\right)\right]\left(\frac{\alpha_s^{(n_l)}(\mu)}{4\pi}\right)^2 + \left[-\frac{1}{6}C_F^3L_\mu^6 + \left(-\frac{5}{2}C_F^3 + \frac{11}{9}C_AC_F^2 - \frac{4}{9}n_lT_FC_F^2\right)L_\mu^5\right. \\
&+ \left(-\frac{121}{54}C_A^2C_F - \frac{70}{9}n_lT_FC_F^2 - \left(\frac{37}{2} + \frac{\pi^2}{12}\right)C_F^3 + \left(\frac{409}{18} - \frac{\pi^2}{3}\right)C_AC_F^2 - \frac{8}{27}n_l^2T_F^2C_F + \frac{44}{27}C_An_lT_FC_F\right)L_\mu^4 \\
&+ \left(\left(24\zeta_3 - \frac{238}{3} - \frac{17\pi^2}{6}\right)C_F^3 - \left(\frac{1540}{27} + \frac{26\pi^2}{27}\right)n_lT_FC_F^2 - \frac{400}{81}n_l^2T_F^2C_F + \left(\frac{4601}{27} + \frac{17\pi^2}{54} - 22\zeta_3\right)C_AC_F^2\right. \\
&+ \left(\frac{2476}{81} - \frac{8\pi^2}{27}\right)C_An_lT_FC_F + \left(\frac{22\pi^2}{27} - \frac{3595}{81}\right)C_A^2C_F\Big)L_\mu^3 + \left(\left(-\frac{6799}{24} + \frac{155\pi^2}{12} + \frac{47\pi^4}{72} - \frac{148}{3}\pi^2\ln(2)\right.\right. \\
&\left.+ 208\zeta_3\right)C_F^3 + \left(\frac{92\zeta_3}{9} - \frac{34205}{162} - \frac{326\pi^2}{27}\right)n_lT_FC_F^2 + \left(\frac{16\zeta_3}{3} - \frac{7126}{81} + \frac{232\pi^2}{27}\right)T_FC_F^2 \\
&+ \left(\frac{483547}{648} + \frac{395\pi^2}{54} - \frac{103\pi^4}{180} + \frac{74}{3}\pi^2\ln(2) - \frac{2260\zeta_3}{9}\right)C_AC_F^2 - \left(\frac{2680}{81} + \frac{32\pi^2}{27}\right)n_l^2T_F^2C_F \\
&+ \left(\frac{220\zeta_3}{3} - \frac{27190}{81} - \frac{14\pi^2}{9} - \frac{11\pi^4}{45}\right)C_A^2C_F + \left(\frac{17956}{81} + \frac{112\pi^2}{27} - \frac{32\zeta_3}{3}\right)C_An_lT_FC_F\Big)L_\mu^2 \\
&+ \left(\left(-\frac{16811}{24} + \frac{393\pi^2}{4} + \frac{479\pi^4}{360} - \frac{740}{3}\pi^2\ln(2) + 660\zeta_3 + \frac{28\pi^2\zeta_3}{3} + 240\zeta_5\right)C_F^3\right. \\
&+ \left(\frac{1479851}{648} - \frac{29185\pi^2}{162} - \frac{2887\pi^4}{540} + \frac{4366}{9}\pi^2\ln(2) - \frac{13106\zeta_3}{9} - 120\zeta_5 - \frac{19\pi^2\zeta_3}{3}\right)C_AC_F^2 \\
&+ \left(\frac{80\zeta_3}{3} - \frac{35630}{81} + \frac{1160\pi^2}{27}\right)T_FC_F^2 + \left(\frac{692\zeta_3}{3} - \frac{86683}{162} + \frac{2812\pi^2}{81} + \frac{16\pi^4}{27} - \frac{1184}{9}\pi^2\ln(2)\right)n_lT_FC_F^2 \\
&+ \left(-\frac{1171918}{729} + \frac{12374\pi^2}{243} + \frac{107\pi^4}{45} - \frac{1628}{9}\pi^2\ln(2) + \frac{18874\zeta_3}{27} - 100\zeta_5 - \frac{56\pi^2\zeta_3}{9}\right)C_A^2C_F \\
&- \left(\frac{83776}{729} + \frac{992\pi^2}{81} + \frac{448\zeta_3}{27}\right)n_l^2T_F^2C_F + \left(\frac{156772}{243} - \frac{5104\pi^2}{81} - \frac{352\zeta_3}{9}\right)C_AT_FC_F \\
&\left.\left.+ \left(\frac{128\zeta_3}{9} - \frac{57008}{243} + \frac{1856\pi^2}{81}\right)n_lT_F^2C_F + \left(\frac{677290}{729} + \frac{4364\pi^2}{243} - \frac{8\pi^4}{9} + \frac{592}{9}\pi^2\ln(2) - \frac{1040\zeta_3}{9}\right)C_An_lT_FC_F\right)L_\mu\right.
\end{aligned}$$

$$
\begin{aligned}
&+\left(\frac{175459\pi^2}{972}-\frac{219365}{486}-\frac{41303\pi^4}{2430}-\frac{3776}{9}\pi^2\ln(2)+\frac{1472}{27}\pi^2\ln^2(2)+\frac{1072\ln^4(2)}{27}+\frac{8576\mathrm{Li}_4(\frac{1}{2})}{9}\right.\\
&\left.+\frac{64816\zeta_3}{81}+\frac{298\pi^2\zeta_3}{9}+\frac{896\zeta_5}{9}\right)C_F^2 n_l T_F+\left(\frac{8584738}{6561}+\frac{151303\pi^2}{2187}+\frac{4703\pi^4}{1215}+\frac{1888}{9}\pi^2\ln(2)-\frac{736}{27}\pi^2\ln^2(2)\right.\\
&\left.-\frac{536\ln^4(2)}{27}-\frac{4288\mathrm{Li}_4(\frac{1}{2})}{9}-\frac{12640\zeta_3}{81}-\frac{76\pi^2\zeta_3}{9}-136\zeta_5\right)C_A C_F n_l T_F-95.129849223056117750 05 C_A C_F T_F\\
&+1429.620347566906229597 83 C_A C_F^2-3126.146253828956158029 02 C_A^2 C_F\\
&+181.977378774929155887 66 C_F^2 T_F+345.533508420189109413 36 C_F^3\\
&+\left(\frac{128\pi^2}{15}-\frac{23936}{81}-\frac{32\pi^4}{135}+\frac{1664\zeta_3}{9}\right)C_F T_F^2+\left(\frac{7088\pi^2}{243}-\frac{211888}{729}-\frac{64\pi^4}{405}+\frac{256\zeta_3}{27}\right)C_F n_l T_F^2\\
&-\left(\frac{741898}{6561}+\frac{6632\pi^2}{243}+\frac{884\pi^4}{1215}+\frac{20672\zeta_3}{243}\right)C_F n_l^2 T_F^2\Bigg]\left(\frac{\alpha_s^{(n_l)}(\mu)}{4\pi}\right)^3+\mathcal{O}(\alpha_s^4). \qquad (50)
\end{aligned}
$$

In this expression, the bottom-quark mass in $L_\mu = \ln(\mu^2/m_b^2)$ is renormalized in the pole scheme. In this scheme, the hard function satisfies the following RGE,

$$
\frac{\mathrm{d}h_s(\mu)}{\mathrm{d}\ln\mu}=\left[-\gamma^{\mathrm{cusp}}(\alpha_s^{(n_l)}(\mu))\ln\frac{\mu^2}{m_b^2}+2\gamma^H(\alpha_s^{(n_l)}(\mu))\right]h_s(\mu). \qquad (51)
$$

At a given order in α_s, all terms containing L_μ are determined by the anomalous dimension coefficients and lower-loop results, and all our L_μ terms agree with the derivation in Ref. [71]. The L_μ-independent terms at three loops are, however, genuinely new. In Eq. (50), all terms through to two loops are analytic and agree with Refs. [61,69–71]. At three loops, all terms containing L_μ, as well as the light fermionic pieces and the color factor $C_F T_F^2$ are also analytic. The remaining ones are obtained numerically to at least 100 decimal digits, of which we display 20 in the present write-up. An electronic version of Eq. (50) can be downloaded from the webpage [164].

Upon substituting the numerical values $C_A = 3$, $C_F = 4/3$, $T_F = 1/2$, and $n_l = 4$ for the color and flavor factors, the expansion of h_s for $\mu = m_b$ reads

$$
\begin{aligned}
h_s(m_b) = 1 &- 4.548311355616075478 8\left(\frac{\alpha_s^{(4)}(m_b)}{\pi}\right)-19.286105172591724459\left(\frac{\alpha_s^{(4)}(m_b)}{\pi}\right)^2\\
&-181.16173810663548219\left(\frac{\alpha_s^{(4)}(m_b)}{\pi}\right)^3+\mathcal{O}(\alpha_s^4). \qquad (52)
\end{aligned}
$$

An interesting detail to note is that the coefficient h_3, which was treated as a nuisance parameter in Ref. [71] and varied in the range $h_3 = 0 \pm 80$, comes out of the genuine three-loop calculation as $h_3 = -181.1617381$ and therefore more than a factor of two larger in magnitude compared to the variation boundaries.

VII. CONCLUSION

We compute the three-loop QCD corrections to heavy-to-light transitions for the entire set of Dirac bilinears which are independent in four space-time dimensions. The calculations use state-of-the art multiloop techniques and a well-established workflow, starting from the generation of the amplitude and the projection onto Lorentz-covariant structures. The resulting scalar integrals are subsequently reduced to master integrals. A certain subset of master integrals (one- and two-loop integrals, three-loop leading color and fermionic integrals apart from the ones with a single closed heavy fermion loop) are obtained analytically, while for the others the differential equations are solved via the "expand and match" method, which uses expansions about several kinematic points and as such gives semianalytic results for the form factors.

Infrared subtraction is applied to the ultraviolet renormalized QCD form factors at three loops, and finite matching coefficients to SCET are obtained. In this procedure, the poles in the dimensional regulator ϵ cancel to at least 12 digits and we thus estimate the precision of the finite part to be at least ten digits. From the matching coefficients of the tensor current at lightlike momentum transfer, the three-loop correction to the hard function in $\bar{B} \to X_s\gamma$ is extracted. Further phenomenological applications to rare semileptonic decays, top-quark or muon decays are left for future investigations.

Electronic results are provided as *Mathematica* and Fortran codes which allow for fast and precise numerical evaluations for physically relevant values of the square of the four-momentum transfer (we do not consider values of $s/m^2 > 1$, though). The supplementary material to this paper can be found on the websites [55,164,167].

ACKNOWLEDGMENTS

We thank Johann Usovitsch and Zihao Wu for allowing us to use the development version of Kira and Ze Long Liu for discussion about the infrared singularity structure. Moreover, we thank Robin Brüser and Maximilian Stahlhofen for collaboration at initial stages and useful correspondence. The research of T. H., J. M., and M. S. was supported by the Deutsche Forschungsgemeinschaft (German Research Foundation) under Grant No. 396021762—TRR 257 "Particle Physics Phenomenology after the Higgs Discovery." K. S. has received funding from the European Research Council (ERC) under the European Union's Horizon 2020 research and innovation programme Grant Agreement No. 101019620 (ERC Advanced Grant TOPUP). The work of M. F. was supported by the European Union's Horizon 2020 research and innovation program under the Marie Skłodowska-Curie Grant Agreement No. 101065445 —PHOBIDE. The work of F. L. was supported by the Swiss National Science Foundation under Contract No. TMSGI2_211209. The Feynman diagrams were drawn with the help of Axodraw [168] and JaxoDraw [169].

APPENDIX A: PROJECTORS

The scalar form factors introduced in Eq. (3) are obtained by the application of the appropriate projectors via

$$F_i^\delta = \mathrm{Tr}[P^\mu_{\delta,i}\Gamma^\delta], \tag{A1}$$

where the $P^\mu_{\delta,i}$ are given by

$$\begin{aligned}
P^\mu_{v,i} &= \not{q}_1\left[g^v_{1,i}\gamma^\mu + g^v_{2,i}\frac{p^\mu}{m} + g^v_{3,i}\frac{q^\mu}{m}\right](\not{q}_2 + m),\\
P^\mu_{a,i} &= \not{q}_1\left[g^a_{1,i}\gamma^\mu + g^a_{2,i}\frac{p^\mu}{m} + g^a_{3,i}\frac{q^\mu}{m}\right]\gamma_5(\not{q}_2 + m),\\
P^s &= \not{q}_1 g_s(\not{q}_2 + m),\\
P^p &= \not{q}_1 \mathrm{i} g_p\gamma_5(\not{q}_2 + m),\\
P^{\mu\nu}_{t,j} &= \not{q}_1\left[g^t_{1,j}\frac{i}{2}\sigma^{\mu\nu} + g^t_{2,j}\frac{q_1^\mu\gamma^\nu - q_1^\nu\gamma^\mu}{m} + g^t_{3,j}\frac{q_2^\mu\gamma^\nu - q_2^\nu\gamma^\mu}{m} + g^t_{4,j}\frac{q_1^\mu q_2^\nu - q_1^\nu q_2^\mu}{m^2}\right](\not{q}_2 + m),
\end{aligned} \tag{A2}$$

with $p = q_1 + q_2$, $q = q_1 - q_2$, $i = 1, 2, 3$, and $j = 1, \ldots, 4$. The coefficients are functions of m, s, and ϵ and read

$$g^v_{1,1} = \frac{s}{4(1-\epsilon)(s-m^2)^2}, \quad g^v_{2,1} = -\frac{(-3+2\epsilon)m^2 s}{4(1-\epsilon)(s-m^2)^3}, \quad g^v_{3,1} = -\frac{m^2(-2m^2+2\epsilon m^2 - s)}{4(1-\epsilon)(s-m^2)^3}, \tag{A3}$$

$$g^v_{1,2} = -\frac{m^2}{4(1-\epsilon)(s-m^2)^2}, \quad g^v_{2,2} = \frac{m^2(-m^2-2s+2\epsilon s)}{4(1-\epsilon)(s-m^2)^3}, \quad g^v_{3,2} = \frac{(-3+2\epsilon)m^4}{4(1-\epsilon)(s-m^2)^3}, \tag{A4}$$

$$g^v_{1,3} = \frac{m^2}{8(1-\epsilon)(s-m^2)^2}, \quad g^v_{2,3} = -\frac{(-3+2\epsilon)m^4}{8(1-\epsilon)(s-m^2)^3}, \quad g^v_{3,3} = -\frac{m^2(-5m^2+4\epsilon m^2+2s-2\epsilon s)}{8(1-\epsilon)(s-m^2)^3}, \tag{A5}$$

$$g^a_{1,1} = \frac{s}{4(1-\epsilon)(s-m^2)^2}, \quad g^a_{2,1} = \frac{(-3+2\epsilon)m^2 s}{4(1-\epsilon)(s-m^2)^3}, \quad g^a_{3,1} = \frac{m^2(-2m^2+2\epsilon m^2 - s)}{4(1-\epsilon)(s-m^2)^3}, \tag{A6}$$

$$g^a_{1,2} = -\frac{m^2}{4(1-\epsilon)(s-m^2)^2}, \quad g^a_{2,2} = -\frac{m^2(-m^2-2s+2\epsilon s)}{4(1-\epsilon)(s-m^2)^3}, \quad g^a_{3,2} = -\frac{(-3+2\epsilon)m^4}{4(1-\epsilon)(s-m^2)^3}, \tag{A7}$$

$$g^a_{1,3} = \frac{m^2}{8(1-\epsilon)(s-m^2)^2}, \qquad g^a_{2,3} = \frac{(-3+2\epsilon)m^4}{8(1-\epsilon)(s-m^2)^3}, \qquad g^a_{3,3} = \frac{m^2(-5m^2+4\epsilon m^2+2s-2\epsilon s)}{8(1-\epsilon)(s-m^2)^3}, \tag{A8}$$

$$g^s = \frac{1}{2(m^2-s)}, \tag{A9}$$

$$g^p = \frac{1}{2(m^2-s)}, \tag{A10}$$

$$g^t_{1,1} = -\frac{1}{2(1-3\epsilon+2\epsilon^2)(m^2-s)}, \quad g^t_{2,1} = \frac{m^2}{2(-1+\epsilon)(-1+2\epsilon)(m^2-s)^2}, \quad g^t_{3,1} = 0, g^t_{4,1} = -\frac{m^2}{2(1-3\epsilon+2\epsilon^2)(m^2-s)^2}, \tag{A11}$$

$$\begin{aligned} g^t_{1,2} &= -\frac{m^2}{(-1+\epsilon)(-1+2\epsilon)(m^2-s)^2}, \qquad g^t_{2,2} = \frac{-(-3+2\epsilon)m^4}{2(-1+\epsilon)(-1+2\epsilon)(m^2-s)^3}, \\ g^t_{3,2} &= \frac{m^2}{4(-1+\epsilon)(m^2-s)^2}, \qquad g^t_{4,2} = -\frac{(-3+2\epsilon)m^4}{2(-1+\epsilon)(-1+2\epsilon)(m^2-s)^3}, \end{aligned} \tag{A12}$$

$$g^t_{1,3} = 0, g^t_{2,3} = \frac{m^2}{4(-1+\epsilon)(m^2-s)^2}, \qquad g^t_{3,3} = 0, g^t_{4,3} = 0, \tag{A13}$$

$$g^t_{1,4} = \frac{m^2}{(1-3\epsilon+2\epsilon^2)(m^2-s)^2}, \qquad g^t_{2,4} = \frac{(-3+2\epsilon)m^4}{2(1-3\epsilon+2\epsilon^2)(m^2-s)^3}, \qquad g^t_{3,4} = 0, g^t_{4,4} = -\frac{\epsilon(-3+2\epsilon)m^4}{(1-3\epsilon+2\epsilon^2)(m^2-s)^3}. \tag{A14}$$

APPENDIX B: IMPLEMENTATION IN COMPUTER CODE

In this appendix we present the implementation of the three-loop form factors for the heavy-to-light transition in the Fortran library FFh2l. The library numerically evaluates the third-order corrections to the form factors. The code is deposited on Zenodo [167] and also available at the web address [55] where documentation and sample programs can be found. The code provides interpolation grids and series expansion which can be used for instance in a Monte Carlo program.

We do not implement all series expansion presented in Eq. (30), instead we use Chebyshev interpolation grids in the range $-75 < s/m^2 < 15/16$. Around the singular points $s/m^2 = 1, -\infty$ we implement the power-log expansions.

The Fortran library FFh2l can be cloned from Gitlab with

```
$ git clone https://gitlab.com/formfactors3l/ffh2l.git
```

A Fortran compiler such as `gfortran` is required. The library can be compiled by running

```
$ ./configure
make
```

Running `make` without further arguments generates the static library `libffh2l.a` which can be linked to the user's program. The module files are located in the directory `modules`. They must be also passed to the compiler. This gives access to the public functions and subroutines. The names of all subroutines start with the suffix `ffh2l_`.

In order to explain the functionality of the library, let us analyze the following sample program which evaluates the vector form factor at three-loops.

```
program example1
  use ffh2l
  implicit none

  double complex :: ff
  double precision :: s = 0.3d0
  integer :: eporder

  print *,"EXAMPLE 1: Numerical evaluation of"
  print *,"the vector form factor F1 at s = 3/10"
  print *,"————————————————————————————————"
  print *,"Default configuration:"
  print *," - nl =4"
  print *," - nh =1"
  print *,""

  do eporder = -6,0
    print *,"F1( s = ",s,", ep = ",eporder," ) = ", ffh2l_veF1(s,eporder)
  enddo

  print *,""
  print *,"Form factor: finite remainder after IR subtraction"
  print *,"F1^fin( s = ",s," ) = ", ffh2l_veF1_fin(s)

end program example1
```

In the preamble of the program, one includes `use ffh2l` to load the respective module. The form factor is computed by the function `ffh2l_veF1(s,eporder)` which returns the corresponding order in ϵ of the ultraviolet renormalized (but not infrared subtracted) form factor $F_1^{v,(3)}$. The result is the third-order correction in the expansion parameter $\alpha_s^{(n_l)}/(4\pi)$, the strong coupling constant renormalized in the $\overline{\text{MS}}$ scheme with the renormalization scale set to the heavy-quark mass: $\mu = m$.

For the other form factors, the user can replace `veF1` in the function name with one of the following: `veF2, veF3, axF1, axF2, axF3, scF1, psF1, teF1, teF2, teF3, teF4`. Note that the form factors `scF1` and `psF1` have been implemented using as renormalization constants for the currents $Z_s = Z_p = Z_m^{\overline{\text{MS}}}$. In addition to the 12 routines aforementioned, the user can utilize `scF1OS` and `psF1OS` to obtain results for the scalar and pseudoscalar form factors with $Z_s = Z_p = Z_m^{\text{OS}}$ for the current renormalization.

The functions return a `double complex` and have the following two inputs:

```
double complex function ffhl2_veF1 (s, eporder)
   double precision, intent(in) :: s
   integer, intent(in) :: eporder
```

The variable `s` is the value of the momentum transfer normalized with respect to the squared quark mass. The order in the dimensional regulator $\epsilon = (4-d)/2$ is set by the integer `eporder`. Only the values `eporder=-6, ... , 0` are valid. These form factors still contain poles since we do not perform the infrared subtraction. In this way, any infrared subtraction scheme can be applied and it is the task of the user to implement it.

For completeness, we also implement the finite remainder at three loops after minimal subtraction of the infrared poles, as described in Sec. II D. In the example above, the finite remainder for the vector form factor $F_1^{v,(3)}$ is obtained using the function `ffh2l_veF1_fin(s)`. It returns the third-order corrections in the expansion parameter $\alpha_s^{(n_l)}/(4\pi)$. Here the strong coupling constant is renormalized in the $\overline{\text{MS}}$ scheme with the renormalization scale $\mu = m$. The finite remainders for the other form factors are obtained substituting `veF1` with one of the following: `veF2, veF3, axF1, axF2, axF3, scF1, psF1, teF1, teF2, teF3, teF4`. Also in this case, the routines with `scF1` and `psF1` correspond to the form factors renormalized with $Z_s = Z_p = Z_m^{\overline{\text{MS}}}$. We provide additionally two routines identified by `scF1OS` and `psF1OS` for the finite remainder of the scalar and pseudoscalar form factors with $Z_s = Z_p = Z_m^{\text{OS}}$.

Each function returns a `double complex` and has the following two inputs:

```
double complex function ffhl2_veF1_fin (s)
   double precision, intent(in) :: s
```

The variable `s` is the value of the momentum transfer normalized with respect to the squared heavy-quark mass.

In the current implementation, the numerical values of the Casimir are hard coded for QCD in the file `ffh2l_global.F90`. We set $C_F = 4/3, C_A = 3, T_F = 1/2$. By default the number of massless and massive quarks are set to $n_l = 4$ and $n_h = 1$, respectively. The user can modify the values, for instance $n_l = 3$ and $n_h = 0$, in the following way:

```
integer :: nl = 3
integer :: nh = 0
call ffh2l_set_nl(nl)
call ffh2l_set_nh(nh)
```

In addition to the Fortran library, we provide also a *Mathematica* interface by making use of Wolfram's MathLink interface (for details on the setup see Ref. [170]). The interface provides a convenient tool for numerical evaluation and cross-check of our results within *Mathematica*. The interface is complied with

```
$ make mathlink
```

To use the library within *Mathematica*, the interface must be loaded:

```
In[] := Install["PATH/ffh2l"]
```

where `PATH/ffh2l` is the location where the MathLink executable `ffh2l` is saved. The ultraviolet renormalized form factors in QCD are evaluated with a call to one of the following functions:

```
FFh2lveF1 FFh2lveF2 FFh2lveF3
FFh2laxF1 FFh2laxF2 FFh2laxF3
FFh2lscF1 FFh2lscF1OS
FFh2lpsF1. FFh2lpsF1OS
FFh2lteF1 FFh2lteF2 FFh2lteF3 FFh2lteF4
```

For instance, the order ϵ^0 in the ultraviolet renormalized form factor $F_1^{v,(3)}$ is obtained with the following command:

```
In[] := s = 3/10;
In[] := eporder = 0;
In[] := FFh2lveF1[s,eporder]
Out[]:= 2439.87
```

The finite remainders of the form factors after infrared subtraction are obtained by calling the functions

```
FFh2lveF1Fin FFh2lveF2Fin FFh2lveF3Fin
FFh2laxF1Fin FFh2laxF2Fin FFh2laxF3Fin
FFh2lscF1Fin FFh2lscF1OSFin
FFh2lpsF1Fin FFh2lpsF1OSFin
FFh2lteF1Fin FFh2lteF2Fin FFh2lteF3Fin
FFh2lteF4Fin
```

For example, the finite remainder of $F_1^{v,(3)}$ is calculated with

```
In[] := s = 3/10;
In[] := FFh2lveF1Fin[s]
Out[]:= -8467.54
```

Also in *Mathematica*, it is possible to modify the default values of n_l and n_h in the following way:

```
In[] := nl=3;
In[] := nh=0;
In[] := FFh2lSetNl[nl]
In[] := FFh2lSetNh[nh]
```


[1] G. Kramer and B. Lampe, Two-jet cross-section in e^+e^- annihilation, Z. Phys. C **34**, 497 (1987).

[2] T. Matsuura and W. L. van Neerven, Second order logarithmic corrections to the Drell–Yan cross-section, Z. Phys. C **38**, 623 (1988).

[3] T. Matsuura, S. C. van der Marck, and W. L. van Neerven, The calculation of the second order soft and virtual contributions to the Drell-Yan cross section, Nucl. Phys. **B319**, 570 (1989).

[4] T. Gehrmann, T. Huber, and D. Maître, Two-loop quark and gluon form-factors in dimensional regularisation, Phys. Lett. B **622**, 295 (2005).

[5] P. A. Baikov, K. G. Chetyrkin, A. V. Smirnov, V. A. Smirnov, and M. Steinhauser, Quark and gluon form factors to three loops, Phys. Rev. Lett. **102**, 212002 (2009).

[6] T. Gehrmann, E. W. N. Glover, T. Huber, N. Ikizlerli, and C. Studerus, Calculation of the quark and gluon form factors to three loops in QCD, J. High Energy Phys. 06 (2010) 094.

[7] R. N. Lee and V. A. Smirnov, Analytic epsilon expansion of three-loop on-shell master integrals up to four-loop transcendentality weight, J. High Energy Phys. 02 (2011) 102.

[8] T. Gehrmann, E. W. N. Glover, T. Huber, N. Ikizlerli, and C. Studerus, The quark and gluon form factors to three loops in QCD through to $O(\epsilon^2)$, J. High Energy Phys. 11 (2010) 102.

[9] J. M. Henn, A. V. Smirnov, V. A. Smirnov, and M. Steinhauser, A planar four-loop form factor and cusp anomalous dimension in QCD, J. High Energy Phys. 05 (2016) 066.

[10] A. von Manteuffel and R. M. Schabinger, Quark and gluon form factors to four-loop order in QCD: The N_f^3 contributions, Phys. Rev. D **95**, 034030 (2017).

[11] J. Henn, R. N. Lee, A. V. Smirnov, V. A. Smirnov, and M. Steinhauser, Four-loop photon quark form factor and cusp anomalous dimension in the large-N_c limit of QCD, J. High Energy Phys. 03 (2017) 139.

[12] R. N. Lee, A. V. Smirnov, V. A. Smirnov, and M. Steinhauser, n_f^2 contributions to fermionic four-loop form factors, Phys. Rev. D **96**, 014008 (2017).

[13] R. N. Lee, A. V. Smirnov, V. A. Smirnov, and M. Steinhauser, Four-loop quark form factor with quartic

fundamental colour factor, J. High Energy Phys. 02 (2019) 172.
[14] A. von Manteuffel and R. M. Schabinger, Quark and gluon form factors in four loop QCD: The N_f^2 and $N_{q\gamma}N_f$ contributions, Phys. Rev. D **99**, 094014 (2019).
[15] A. von Manteuffel and R. M. Schabinger, Planar master integrals for four-loop form factors, J. High Energy Phys. 05 (2019) 073.
[16] A. von Manteuffel, E. Panzer, and R. M. Schabinger, Cusp and collinear anomalous dimensions in four-loop QCD from form factors, Phys. Rev. Lett. **124**, 162001 (2020).
[17] R. N. Lee, A. von Manteuffel, R. M. Schabinger, A. V. Smirnov, V. A. Smirnov, and M. Steinhauser, Fermionic corrections to quark and gluon form factors in four-loop QCD, Phys. Rev. D **104**, 074008 (2021).
[18] R. N. Lee, A. von Manteuffel, R. M. Schabinger, A. V. Smirnov, V. A. Smirnov, and M. Steinhauser, Quark and gluon form factors in four-loop QCD, Phys. Rev. Lett. **128**, 212002 (2022).
[19] A. Chakraborty, T. Huber, R. N. Lee, A. von Manteuffel, R. M. Schabinger, A. V. Smirnov, and M. Steinhauser, Hbb vertex at four loops and hard matching coefficients in SCET for various currents, Phys. Rev. D **106**, 074009 (2022).
[20] R. Barbieri, J. A. Mignaco, and E. Remiddi, Electron form factors up to fourth order.—I, Nuovo Cimento A **11**, 824 (1972).
[21] R. Barbieri, J. A. Mignaco, and E. Remiddi, Electron form factors up to fourth order.—II, Nuovo Cimento A **11**, 865 (1972).
[22] P. Mastrolia and E. Remiddi, Two loop form-factors in QED, Nucl. Phys. **B664**, 341 (2003).
[23] R. Bonciani, P. Mastrolia, and E. Remiddi, QED vertex form-factors at two loops, Nucl. Phys. **B676**, 399 (2004).
[24] W. Bernreuther, R. Bonciani, T. Gehrmann, R. Heinesch, T. Leineweber, P. Mastrolia, and E. Remiddi, Two-loop QCD corrections to the heavy quark form-factors: The vector contributions, Nucl. Phys. **B706**, 245 (2005).
[25] W. Bernreuther, R. Bonciani, T. Gehrmann, R. Heinesch, T. Leineweber, P. Mastrolia, and E. Remiddi, Two-loop QCD corrections to the heavy quark form factors: Axial vector contributions, Nucl. Phys. **B712**, 229 (2005).
[26] W. Bernreuther, R. Bonciani, T. Gehrmann, R. Heinesch, T. Leineweber, and E. Remiddi, Two-loop QCD corrections to the heavy quark form factors: Anomaly contributions, Nucl. Phys. **B723**, 91 (2005).
[27] W. Bernreuther, R. Bonciani, T. Gehrmann, R. Heinesch, P. Mastrolia, and E. Remiddi, Decays of scalar and pseudoscalar Higgs bosons into fermions: Two-loop QCD corrections to the Higgs-quark-antiquark amplitude, Phys. Rev. D **72**, 096002 (2005).
[28] J. Gluza, A. Mitov, S. Moch, and T. Riemann, The QCD form factor of heavy quarks at NNLO, J. High Energy Phys. 07 (2009) 001.
[29] J. Henn, A. V. Smirnov, V. A. Smirnov, and M. Steinhauser, Massive three-loop form factor in the planar limit, J. High Energy Phys. 01 (2017) 074.
[30] T. Ahmed, J. M. Henn, and M. Steinhauser, High energy behaviour of form factors, J. High Energy Phys. 06 (2017) 125.
[31] J. Ablinger, A. Behring, J. Blümlein, G. Falcioni, A. De Freitas, P. Marquard, N. Rana, and C. Schneider, Heavy quark form factors at two loops, Phys. Rev. D **97**, 094022 (2018).
[32] R. N. Lee, A. V. Smirnov, V. A. Smirnov, and M. Steinhauser, Three-loop massive form factors: Complete light-fermion corrections for the vector current, J. High Energy Phys. 03 (2018) 136.
[33] R. N. Lee, A. V. Smirnov, V. A. Smirnov, and M. Steinhauser, Three-loop massive form factors: Complete light-fermion and large-N_c corrections for vector, axial-vector, scalar and pseudo-scalar currents, J. High Energy Phys. 05 (2018) 187.
[34] J. Ablinger, J. Blümlein, P. Marquard, N. Rana, and C. Schneider, Heavy quark form factors at three loops in the planar limit, Phys. Lett. B **782**, 528 (2018).
[35] J. Ablinger, J. Blümlein, P. Marquard, N. Rana, and C. Schneider, Automated solution of first order factorizable systems of differential equations in one variable, Nucl. Phys. **B939**, 253 (2019).
[36] J. Blümlein, P. Marquard, N. Rana, and C. Schneider, The heavy fermion contributions to the massive three loop form factors, Nucl. Phys. **B949**, 114751 (2019).
[37] J. Blümlein, A. De Freitas, P. Marquard, N. Rana, and C. Schneider, Analytic results on the massive three-loop form factors: Quarkonic contributions, Phys. Rev. D **108**, 094003 (2023).
[38] M. Fael, F. Lange, K. Schönwald, and M. Steinhauser, Massive vector form factors to three loops, Phys. Rev. Lett. **128**, 172003 (2022).
[39] M. Fael, F. Lange, K. Schönwald, and M. Steinhauser, Singlet and nonsinglet three-loop massive form factors, Phys. Rev. D **106**, 034029 (2022).
[40] M. Fael, F. Lange, K. Schönwald, and M. Steinhauser, Massive three-loop form factors: Anomaly contribution, Phys. Rev. D **107**, 094017 (2023).
[41] S. M. Berman and A. Sirlin, Some considerations on the radiative corrections to muon and neutron decay, Ann. Phys. (N.Y.) **20**, 20 (1962).
[42] C. Anastasiou, K. Melnikov, and F. Petriello, The electron energy spectrum in muon decay through $\mathcal{O}(\alpha^2)$, J. High Energy Phys. 09 (2007) 014.
[43] R. Bonciani and A. Ferroglia, Two-loop QCD corrections to the heavy-to-light quark decay, J. High Energy Phys. 11 (2008) 065.
[44] H. M. Asatrian, C. Greub, and B. D. Pecjak, Next-to-next-to-leading order corrections to $\bar{B} \to X_u \ell \bar{\nu}$ in the shape-function region, Phys. Rev. D **78**, 114028 (2008).
[45] M. Beneke, T. Huber, and X.-Q. Li, Two-loop QCD correction to differential semi-leptonic $b \to u$ decays in the shape-function region, Nucl. Phys. **B811**, 77 (2009).
[46] G. Bell, NNLO corrections to inclusive semileptonic B decays in the shape-function region, Nucl. Phys. **B812**, 264 (2009).
[47] G. Bell, Higher order QCD corrections in exclusive charmless B decays, Ph.D. thesis, Munich University, 2006.
[48] G. Bell, NNLO vertex corrections in charmless hadronic B decays: Imaginary part, Nucl. Phys. **B795**, 1 (2008).

[49] T. Huber, On a two-loop crossed six-line master integral with two massive lines, J. High Energy Phys. 03 (2009) 024.

[50] L.-B. Chen, Two-loop master integrals for heavy-to-light form factors of two different massive fermions, J. High Energy Phys. 02 (2018) 066.

[51] T. Engel, C. Gnendiger, A. Signer, and Y. Ulrich, Small-mass effects in heavy-to-light form factors, J. High Energy Phys. 02 (2019) 118.

[52] L.-B. Chen and J. Wang, Three-loop planar master integrals for heavy-to-light form factors, Phys. Lett. B **786**, 453 (2018).

[53] S. Datta, N. Rana, V. Ravindran, and R. Sarkar, Three loop QCD corrections to the heavy-light form factors in the color-planar limit, J. High Energy Phys. 12 (2023) 001.

[54] M. Fael, F. Lange, K. Schönwald, and M. Steinhauser, A semi-analytic method to compute Feynman integrals applied to four-loop corrections to the $\overline{\text{MS}}$-pole quark mass relation, J. High Energy Phys. 09 (2021) 152.

[55] https://gitlab.com/formfactors3l/ffh2l/.

[56] C. W. Bauer, S. Fleming, D. Pirjol, and I. W. Stewart, An effective field theory for collinear and soft gluons: Heavy to light decays, Phys. Rev. D **63**, 114020 (2001).

[57] C. W. Bauer, D. Pirjol, and I. W. Stewart, Soft-collinear factorization in effective field theory, Phys. Rev. D **65**, 054022 (2002).

[58] M. Beneke, A. P. Chapovsky, M. Diehl, and T. Feldmann, Soft-collinear effective theory and heavy-to-light currents beyond leading power, Nucl. Phys. **B643**, 431 (2002).

[59] M. Beneke and T. Feldmann, Multipole-expanded soft-collinear effective theory with non-Abelian gauge symmetry, Phys. Lett. B **553**, 267 (2003).

[60] S. W. Bosch, B. O. Lange, M. Neubert, and G. Paz, Factorization and shape-function effects in inclusive B-meson decays, Nucl. Phys. **B699**, 335 (2004).

[61] G. Bell, M. Beneke, T. Huber, and X.-Q. Li, Heavy-to-light currents at NNLO in SCET and semi-inclusive $\bar{B} \to X_s l^+ l^-$ decay, Nucl. Phys. **B843**, 143 (2011).

[62] G. P. Korchemsky and G. F. Sterman, Infrared factorization in inclusive B meson decays, Phys. Lett. B **340**, 96 (1994).

[63] R. Akhoury and I. Z. Rothstein, Extraction of V_{ub} from inclusive B decays and the resummation of end point logarithms, Phys. Rev. D **54**, 2349 (1996).

[64] M. Neubert, Renormalization-group improved calculation of the $B \to X_s\gamma$ branching ratio, Eur. Phys. J. C **40**, 165 (2005).

[65] T. Becher and M. Neubert, Toward a NNLO calculation of the $\bar{B} \to X_s\gamma$ decay rate with a cut on photon energy: I. Two-loop result for the soft function, Phys. Lett. B **633**, 739 (2006).

[66] T. Becher and M. Neubert, Toward a NNLO calculation of the $\bar{B} \to X_s\gamma$ decay rate with a cut on photon energy: II. Two-loop result for the jet function, Phys. Lett. B **637**, 251 (2006).

[67] R. Brüser, Z. L. Liu, and M. Stahlhofen, Three-loop quark jet function, Phys. Rev. Lett. **121**, 072003 (2018).

[68] R. Brüser, Z. L. Liu, and M. Stahlhofen, Three-loop soft function for heavy-to-light quark decays, J. High Energy Phys. 03 (2020) 071.

[69] A. Ali, B. D. Pecjak, and C. Greub, $B \to V\gamma$ decays at NNLO in SCET, Eur. Phys. J. C **55**, 577 (2008).

[70] Z. Ligeti, I. W. Stewart, and F. J. Tackmann, Treating the b quark distribution function with reliable uncertainties, Phys. Rev. D **78**, 114014 (2008).

[71] B. Dehnadi, I. Novikov, and F. J. Tackmann, The photon energy spectrum in $B \to X_s\gamma$ at $\text{N}^3\text{LL}'$, J. High Energy Phys. 07 (2023) 214.

[72] D. R. T. Jones, Two-loop diagrams in Yang-Mills theory, Nucl. Phys. **B75**, 531 (1974).

[73] W. E. Caswell, Asymptotic behavior of non-Abelian gauge theories to two-loop order, Phys. Rev. Lett. **33**, 244 (1974).

[74] E. Egorian and O. V. Tarasov, Two loop renormalization of the QCD in an arbitrary gauge, Teor. Mat. Fiz. **41**, 26 (1979).

[75] R. Tarrach, The pole mass in perturbative QCD, Nucl. Phys. **B183**, 384 (1981).

[76] N. Gray, D. J. Broadhurst, W. Grafe, and K. Schilcher, Three-loop relation of quark $\overline{\text{MS}}$ and pole masses, Z. Phys. C **48**, 673 (1990).

[77] K. G. Chetyrkin and M. Steinhauser, Short-distance mass of a heavy quark at order α_s^3, Phys. Rev. Lett. **83**, 4001 (1999).

[78] K. G. Chetyrkin and M. Steinhauser, The relation between the $\overline{\text{MS}}$ and the on-shell quark mass at order α_s^3, Nucl. Phys. **B573**, 617 (2000).

[79] K. Melnikov and T. van Ritbergen, The three-loop relation between the $\overline{\text{MS}}$ and the pole quark masses, Phys. Lett. B **482**, 99 (2000).

[80] P. Marquard, A. V. Smirnov, V. A. Smirnov, M. Steinhauser, and D. Wellmann, $\overline{\text{MS}}$-on-shell quark mass relation up to four loops in QCD and a general $\text{SU}(N)$ gauge group, Phys. Rev. D **94**, 074025 (2016).

[81] D. J. Broadhurst, N. Gray, and K. Schilcher, Gauge-invariant on-shell Z_2 in QED, QCD and the effective field theory of a static quark, Z. Phys. C **52**, 111 (1991).

[82] K. Melnikov and T. van Ritbergen, The three-loop on-shell renormalization of QCD and QED, Nucl. Phys. **B591**, 515 (2000).

[83] P. Marquard, L. Mihaila, J. H. Piclum, and M. Steinhauser, Relation between the pole and the minimally subtracted mass in dimensional regularization and dimensional reduction to three-loop order, Nucl. Phys. **B773**, 1 (2007).

[84] P. Marquard, A. V. Smirnov, V. A. Smirnov, and M. Steinhauser, Four-loop wave function renormalization in QCD and QED, Phys. Rev. D **97**, 054032 (2018).

[85] K. G. Chetyrkin, B. A. Kniehl, and M. Steinhauser, Decoupling relations to $O(\alpha_s^3)$ and their connection to low-energy theorems, Nucl. Phys. **B510**, 61 (1998).

[86] M. Gerlach, F. Herren, and M. Steinhauser, Wilson coefficients for Higgs boson production and decoupling relations to $\mathcal{O}(\alpha_s^4)$, J. High Energy Phys. 11 (2018) 141.

[87] O. V. Tarasov, Anomalous dimensions of quark masses in the three-loop approximation, Phys. Part. Nucl. Lett. **17**, 109 (2020).

[88] S. A. Larin, The renormalization of the axial anomaly in dimensional regularization, Phys. Lett. B **303**, 113 (1993).

[89] D. J. Broadhurst and A. G. Grozin, Matching QCD and heavy-quark effective theory heavy-light currents at two loops and beyond, Phys. Rev. D **52**, 4082 (1995).

[90] J. A. Gracey, Three loop $\overline{\text{MS}}$ tensor current anomalous dimension in QCD, Phys. Lett. B **488**, 175 (2000).

[91] S. Weinberg, Effective gauge theories, Phys. Lett. **91B**, 51 (1980).
[92] B. A. Ovrut and H. J. Schnitzer, Gauge theories with minimal subtraction and the decoupling theorem, Nucl. Phys. **B179**, 381 (1981).
[93] B. A. Ovrut and H. J. Schnitzer, Gauge theory and effective Lagrangian, Nucl. Phys. **B189**, 509 (1981).
[94] W. Wetzel, Minimal subtraction and the decoupling of heavy quarks for arbitrary values of the gauge parameter, Nucl. Phys. **B196**, 259 (1982).
[95] W. Bernreuther and W. Wetzel, Decoupling of heavy quarks in the minimal subtraction scheme, Nucl. Phys. **B197**, 228 (1982).
[96] W. Bernreuther, Decoupling of heavy quarks in quantum chromodynamics, Ann. Phys. (N.Y.) **151**, 127 (1983).
[97] Y. Schröder and M. Steinhauser, Four-loop decoupling relations for the strong coupling, J. High Energy Phys. 01 (2006) 051.
[98] K. G. Chetyrkin, J. H. Kühn, and C. Sturm, QCD decoupling at four loops, Nucl. Phys. **B744**, 121 (2006).
[99] A. G. Grozin, P. Marquard, J. H. Piclum, and M. Steinhauser, Three-loop chromomagnetic interaction in HQET, Nucl. Phys. **B789**, 277 (2008).
[100] A. G. Grozin, M. Höschele, J. Hoff, and M. Steinhauser, Simultaneous decoupling of bottom and charm quarks, J. High Energy Phys. 09 (2011) 066.
[101] T. Becher and M. Neubert, Infrared singularities of QCD amplitudes with massive partons, Phys. Rev. D **79**, 125004 (2009).
[102] Z. L. Liu and N. Schalch, Infrared singularities of multileg QCD amplitudes with a massive parton at three loops, Phys. Rev. Lett. **129**, 232001 (2022).
[103] S. Moch, J. A. M. Vermaseren, and A. Vogt, The three-loop splitting functions in QCD: The non-singlet case, Nucl. Phys. **B688**, 101 (2004).
[104] J. Davies, A. Vogt, B. Ruijl, T. Ueda, and J. A. M. Vermaseren, Large-n_f contributions to the four-loop splitting functions in QCD, Nucl. Phys. **B915**, 335 (2017).
[105] S. Moch, B. Ruijl, T. Ueda, J. A. M. Vermaseren, and A. Vogt, Four-loop non-singlet splitting functions in the planar limit and beyond, J. High Energy Phys. 10 (2017) 041.
[106] A. Grozin, Four-loop cusp anomalous dimension in QED, J. High Energy Phys. 06 (2018) 073.
[107] S. Moch, B. Ruijl, T. Ueda, J. A. M. Vermaseren, and A. Vogt, On quartic colour factors in splitting functions and the gluon cusp anomalous dimension, Phys. Lett. B **782**, 627 (2018).
[108] J. M. Henn, T. Peraro, M. Stahlhofen, and P. Wasser, Matter dependence of the four-loop cusp anomalous dimension, Phys. Rev. Lett. **122**, 201602 (2019).
[109] J. M. Henn, G. P. Korchemsky, and B. Mistlberger, The full four-loop cusp anomalous dimension in $\mathcal{N}=4$ super Yang-Mills and QCD, J. High Energy Phys. 04 (2020) 018.
[110] B. Agarwal, A. von Manteuffel, E. Panzer, and R. M. Schabinger, Four-loop collinear anomalous dimensions in QCD and $\mathcal{N}=4$ super Yang-Mills, Phys. Lett. B **820**, 136503 (2021).
[111] S.-O. Moch, J. A. M. Vermaseren, and A. Vogt, The quark form factor at higher orders, J. High Energy Phys. 08 (2005) 049.
[112] S. Moch, J. A. M. Vermaseren, and A. Vogt, Three-loop results for quark and gluon form-factors, Phys. Lett. B **625**, 245 (2005).
[113] G. P. Korchemsky and A. V. Radyushkin, Renormalization of the Wilson loops beyond the leading order, Nucl. Phys. **B283**, 342 (1987).
[114] G. P. Korchemsky and A. V. Radyushkin, Infrared factorization, Wilson lines and the heavy quark limit, Phys. Lett. B **279**, 359 (1992).
[115] N. Kidonakis, Two-loop soft anomalous dimensions and next-to-next-to-leading-logarithm resummation for heavy quark production, Phys. Rev. Lett. **102**, 232003 (2009).
[116] A. Grozin, J. M. Henn, G. P. Korchemsky, and P. Marquard, Three loop cusp anomalous dimension in QCD, Phys. Rev. Lett. **114**, 062006 (2015).
[117] A. G. Grozin, J. M. Henn, G. P. Korchemsky, and P. Marquard, The three-loop cusp anomalous dimension in QCD and its supersymmetric extensions, J. High Energy Phys. 01 (2016) 140.
[118] P. Nogueira, Automatic Feynman graph generation, J. Comput. Phys. **105**, 279 (1993).
[119] M. Gerlach, F. Herren, and M. Lang, TAPIR: A tool for topologies, amplitudes, partial fraction decomposition and input for reductions, Comput. Phys. Commun. **282**, 108544 (2023).
[120] R. Harlander, T. Seidensticker, and M. Steinhauser, Corrections of $\mathcal{O}(\alpha\alpha_s)$ to the decay of the Z boson into bottom quarks, Phys. Lett. B **426**, 125 (1998).
[121] T. Seidensticker, Automatic application of successive asymptotic expansions of Feynman diagrams, in *Proceedings of the 6th International Workshop on New Computing Techniques in Physics Research: Software Engineering, Artificial Intelligence Neural Nets, Genetic Algorithms, Symbolic Algebra, Automatic Calculation* (1999), arXiv:hep-ph/9905298.
[122] J. A. M. Vermaseren, New features of FORM, arXiv:math-ph/0010025.
[123] B. Ruijl, T. Ueda, and J. Vermaseren, FORM version 4.2, arXiv:1707.06453.
[124] P. Maierhöfer, J. Usovitsch, and P. Uwer, Kira—A Feynman integral reduction program, Comput. Phys. Commun. **230**, 99 (2018).
[125] J. Klappert, F. Lange, P. Maierhöfer, and J. Usovitsch, Integral reduction with Kira 2.0 and finite field methods, Comput. Phys. Commun. **266**, 108024 (2021).
[126] J. Klappert and F. Lange, Reconstructing rational functions with FireFly, Comput. Phys. Commun. **247**, 106951 (2020).
[127] J. Klappert, S. Y. Klein, and F. Lange, Interpolation of dense and sparse rational functions and other improvements in FireFly, Comput. Phys. Commun. **264**, 107968 (2021).
[128] F. V. Tkachov, A theorem on analytical calculability of 4-loop renormalization group functions, Phys. Lett. **100B**, 65 (1981).
[129] K. G. Chetyrkin and F. V. Tkachov, Integration by parts: The algorithm to calculate β-functions in 4 loops, Nucl. Phys. **B192**, 159 (1981).

[130] T. Gehrmann and E. Remiddi, Differential equations for two-loop four-point functions, Nucl. Phys. **B580**, 485 (2000).

[131] S. Laporta, High-precision calculation of multiloop Feynman integrals by difference equations, Int. J. Mod. Phys. A **15**, 5087 (2000).

[132] R. Lewis, Fermat, https://home.bway.net/lewis.

[133] A. V. Smirnov and V. A. Smirnov, How to choose master integrals, Nucl. Phys. **B960**, 115213 (2020).

[134] J. Usovitsch, Factorization of denominators in integration-by-parts reductions, arXiv:2002.08173.

[135] M. Kauers, Fast solvers for dense linear systems, Nucl. Phys. B, Proc. Suppl. **183**, 245 (2008).

[136] A. von Manteuffel and R. M. Schabinger, A novel approach to integration by parts reduction, Phys. Lett. B **744**, 101 (2015).

[137] T. Peraro, Scattering amplitudes over finite fields and multivariate functional reconstruction, J. High Energy Phys. 12 (2016) 030.

[138] M. Driesse, G. U. Jakobsen, G. Mogull, J. Plefka, B. Sauer, and J. Usovitsch, Conservative black hole scattering at fifth post-Minkowskian and first self-force order, Phys. Rev. Lett. **132**, 241402 (2024).

[139] R. N. Lee, Presenting LiteRed: A tool for the Loop InTEgrals REDuction, arXiv:1212.2685.

[140] R. N. Lee, LiteRed 1.4: A powerful tool for reduction of multiloop integrals, J. Phys. Conf. Ser. **523**, 012059 (2014).

[141] A. V. Kotikov, Differential equations method. New technique for massive Feynman diagram calculation, Phys. Lett. B **254**, 158 (1991).

[142] A. V. Kotikov, Differential equations method: The calculation of vertex-type Feynman diagrams, Phys. Lett. B **259**, 314 (1991).

[143] A. V. Kotikov, Differential equation method. The calculation of N-point Feynman diagrams, Phys. Lett. B **267**, 123 (1991).

[144] E. Remiddi, Differential equations for Feynman graph amplitudes, Nuovo Cimento A **110**, 1435 (1997).

[145] C. Schneider, Symbolic summation assists combinatorics, Semin. Lotharingien Comb. **56**, 1 (2007).

[146] C. Schneider, *Term Algebras, Canonical Representations and Difference Ring Theory for Symbolic Summation* (Springer International Publishing, Cham, 2021), pp. 423–485, 10.1007/978-3-030-80219-6_17.

[147] J. Blümlein and S. Kurth, Harmonic sums and Mellin transforms up to two-loop order, Phys. Rev. D **60**, 014018 (1999).

[148] J. A. M. Vermaseren, Harmonic sums, Mellin transforms and integrals, Int. J. Mod. Phys. A **14**, 2037 (1999).

[149] J. Blümlein, Structural relations of harmonic sums and Mellin transforms up to weight $w = 5$, Comput. Phys. Commun. **180**, 2218 (2009).

[150] J. Ablinger, A computer algebra toolbox for harmonic sums related to particle physics, Master's thesis, Linz University, 2009.

[151] J. Ablinger, J. Blümlein, and C. Schneider, Harmonic sums and polylogarithms generated by cyclotomic polynomials, J. Math. Phys. (N.Y.) **52**, 102301 (2011).

[152] J. Ablinger, Computer algebra algorithms for special functions in particle physics, Ph.D. thesis, Linz University, 4, 2012.

[153] J. Ablinger, J. Blümlein, and C. Schneider, Generalized harmonic, cyclotomic, and binomial sums, their polylogarithms and special numbers, J. Phys. Conf. Ser. **523**, 012060 (2014).

[154] J. Ablinger, J. Blümlein, and C. Schneider, Analytic and algorithmic aspects of generalized harmonic sums and polylogarithms, J. Math. Phys. (N.Y.) **54**, 082301 (2013).

[155] J. Ablinger, J. Blümlein, C. G. Raab, and C. Schneider, Iterated binomial sums and their associated iterated integrals, J. Math. Phys. (N.Y.) **55**, 112301 (2014).

[156] J. Ablinger, The package HarmonicSums: Computer algebra and analytic aspects of nested sums, Proc. Sci. LL2014 (**2014**) 019 [arXiv:1407.6180].

[157] J. Ablinger, Discovering and proving infinite binomial sums identities, Exp. Math. **26**, 62 (2016).

[158] J. Ablinger, Computing the inverse Mellin transform of holonomic sequences using Kovacic's algorithm, Proc. Sci. RADCOR2017 (**2018**) 001 [arXiv:1801.01039].

[159] H. Ferguson and D. Bailey, A polynomial time, numerically stable integer relation algorithm, Supercomputing Research Center RNR Technical Report No. RNR-91-032.

[160] X. Liu and Y.-Q. Ma, AMFLow: A *Mathematica* package for Feynman integrals computation via auxiliary mass flow, Comput. Phys. Commun. **283**, 108565 (2023).

[161] X. Liu, Y.-Q. Ma, and C.-Y. Wang, A systematic and efficient method to compute multi-loop master integrals, Phys. Lett. B **779**, 353 (2018).

[162] X. Liu and Y.-Q. Ma, Multiloop corrections for collider processes using auxiliary mass flow, Phys. Rev. D **105**, L051503 (2022).

[163] Z.-F. Liu and Y.-Q. Ma, Determining Feynman integrals with only input from linear algebra, Phys. Rev. Lett. **129**, 222001 (2022).

[164] https://www.ttp.kit.edu/preprints/2024/ttp24-017/.

[165] C. Bauer, A. Frink, and R. Kreckel, Introduction to the GiNaC framework for symbolic computation within the C++ programming language, J. Symb. Comput. **33**, 1 (2002).

[166] J. Vollinga and S. Weinzierl, Numerical evaluation of multiple polylogarithms, Comput. Phys. Commun. **167**, 177 (2005).

[167] https://zenodo.org/records/11046426.

[168] J. A. M. Vermaseren, Axodraw, Comput. Phys. Commun. **83**, 45 (1994).

[169] D. Binosi and L. Theußl, JaxoDraw: A graphical user interface for drawing Feynman diagrams, Comput. Phys. Commun. **161**, 76 (2004).

[170] T. Hahn, The high-energy physicist's guide to MathLink, Comput. Phys. Commun. **183**, 460 (2012).